AIAA SciTech Forum
8–12 January 2018, Kissimmee, Florida
2018 AIAA Aerospace Sciences Meeting

10.2514/6.2018-0143

Investigation of Dataset Construction Parameters and their Impact on Reaction Model Optimization using PrIMe

A. Mirzayeva[1], N.A. Slavinskaya [2], U. Riedel[3]
Institute of Combustion Technology, German Aerospace Center (DLR), Stuttgart, 70569, Germany

M. Frenklach[4], A. Packard [5], W. Li[6], J. Oreluk[7], A. Hegde[8]
Department of Mechanical Engineering, University of California, Berkeley, CA 94720, USA

The current paper presents a continuation of the development of a modern methodology for the construction of uncertainty-quantified chemical reaction models on the base of the Bound-to-Bound Data Collaboration (B2BDC) module of the automated data-centric infrastructure PrIMe. Some problems, postulated in the recent studies, are in the focus of the present investigation. The question of targets amount (experimental data, Quantities of Interest (QoI)) selected for the analysis has been studied. To investigate this, the PrIMe dataset is augmented. The influence of dataset extension on the dataset consistency, feasible parameter set, and model optimization is studied and an algorithm for the selection of QoI in each experimental set is postulated. The approach of combined methods of scalar consistency measure, SCM, and vector consistency measure, VCM, for consistency analysis are adapted and successfully implemented. Predictions of the LS-$\mathcal{F}$ optimized mechanism are compared against a wide range of experimental data of laminar premixed flames and shock tube ignition delay times. Good agreement of model predictions with the experimental measurements is obtained.

Nomenclature

ϕ	=	equivalence ratio
P_5	=	pressure behind reflected shock waves in shock-tube experiments
QoI	=	quantity of interest
T_5	=	temperature behind reflected shock waves in shock-tube experiments
T_0	=	initial temperature in laminar flame experiments
UB	=	uncertainty bounds

I. Introduction

ONE of the most important properties of a reaction model in chemical engineering is to make predictions about the system when certain settings are changed. Appropriate handling and archiving of experimental data from different sources, and of the many uncertainties in the data embedded in the kinetic models, is a major challenge the chemical kinetics community has to tackle before becoming a predictive science. Methods for determining whether or not the model predictions are consistent with experimental data have been of great interest in combustion research over decades. Developing predictive models[1] has become the goal in many of the modelling studies on reaction systems. Numerical optimization of complex reaction networks, of the kind that guided the development of GRI-Mech,[1-3] e.g., has now been accepted as one of the underlying methods in this pursuit.[4-6] In order to develop a

[1] PhD Student, Chemical Kinetics Department, Aziza.Mirzayeva@dlr.de
[2] Senior research fellow, Chemical Kinetics Department, Nadja.Slavinskaya@dlr.de, AIAA Senior Member
[3] Head of Chemical Kinetics Department, Uwe.Riedel@dlr.de, AIAA Senior Member
[4] Prof. of University of California, Berkeley, frenklach@berkeley.edu, AIAA Member
[5] Prof. of University of California, Berkeley, apackard@berkeley.edu.
[6] PhD Student of University of California, Berkeley, wenyuli@berkeley.edu.
[7] PhD Student of University of California, Berkeley, jim.oreluk@berkeley.edu.
[8] PhD Student of University of California, Berkeley, arun.hegde@berkeley.edu.

predictive reaction model for complex chemical systems the integration of large amounts of theoretical, computational, and experimental data collected by numerous researchers is required. The integration of such data entails assessment of the consistency of the data, validation of models, and quantification of uncertainties for model predictions and often requires calibrating unknown parameters based on experimental observations.

The interest for development of chemical models spurred the interest in the quality of experimental data, i.e. uncertainty quantification. There has been plenty of research on data collaboration over the years;[1,2,7-9] this also led to the development of cybersystems offering kinetic database platforms, calculation and data analysis tools. Based on a long research on such cybersystems, we chose an automated data-centric infrastructure, the Process Informatics Model (PrIMe)[7] and tested it on the updated version of hydrogen/syngas reaction model published in Slavinskaya et al.[10]

II. Theoretical background

B2BDC is a computational framework developed for a treatment of collective information content (combined numerical and experimental data) collected from multiple sources.[1,2,8,11-14] This approach allows the users to investigate the studied data consistency, identify the sources of inconsistency, evaluate (and re-evaluate) data uncertainty and optimize models under development. The main steps of the B2BDC methodology for the UQ reaction model analysis are dataset construction, feasible set computation, data consistency analysis and final model optimizations.

A *dataset* is a collection of model-data constraints where uncertain model parameters, with prior ranges $\{l_i \leq x_i \leq u_i\}_{i=1}^{n}$, are constrained by both models $\{M_e(x)\}_{e=1}^{N}$ and experimental observations, or *Quantities of Interest* (QoIs), given on the uncertainty interval, [L_e , U_e] for each *e*-th QoI.[13-15] These models generally take the form of surrogates and map to observed experimental targets. Let the hyper-rectangle $\mathcal{H}$ define the prior uncertainty for the model parameters. For each individual QoI, we can find a feasible set of parameters on which the corresponding surrogate model matches the experimental bounds:

$$\mathcal{F}_e := \{x \in \mathcal{H} : L_e \leq M_e(x) \leq U_e\} \tag{1}$$

The feasible set of the dataset is defined as follows:

$$\mathcal{F} := \cap_{e=1}^{N} \mathcal{F}_e = \{x \in \mathcal{H} : L_e \leq M_e(x) \leq U_e, for\ e = 1, .., N\} \tag{2}$$

i.e., the collection of all parameters for which model predictions match experimental bounds. If the feasible set is nonempty, the dataset is said to be *consistent*. Conversely, if the feasible set is empty, i.e. *inconsistent*, then there is disagreement between models and data: no parameter vector can satisfy all model-data constraints. Inconsistency can often be attributed to misspecified experimental observations, incorrect model forms, or a combination of both.

Consistency analysis is a key unit of any dataset. If a dataset is defined to be inconsistent, no further analysis can be performed. Moreover, consistency of a dataset allows minimizing the error propagation. Therefore, prior to any model optimization and improvement, it is necessary to investigate the role of consistency analysis in the model optimization and influence of consistency assessment processes on the model output.

The B2BDC methodology offers two kinds of consistency analysis measures: SCM, namely scalar consistency measure, and VCM, vector consistency measure. In earlier work by R. Feeley and coworkers,[11] a quantitative measure of dataset consistency was proposed as follows:

$$\begin{aligned} \text{SCM:} \quad &= \max_{x \in \mathcal{H}, \gamma} \gamma \\ \text{s.t.} \quad & (1-\gamma)\tfrac{L_e - U_e}{2} \leq M_e(x) - \tfrac{U_e + L_e}{2} \leq (1-\gamma)\tfrac{U_e - L_e}{2} \quad for\ e = 1, \ldots, N \end{aligned} \tag{3}$$

In recent work,[16] this measure was termed the *scalar consistency measure (SCM)*. Loosely speaking, the SCM provides the maximal allowable symmetric tightening of all model-data constraints. Hence, if the SCM is positive, the dataset is consistent. If the SCM is negative, then the dataset is inconsistent. In the case of inconsistent datasets, sensitivity calculations for the SCM provide a means of identifying possible problematic model-data constraints. Strategies for resolving inconsistent datasets using this technique are described in references.[11,16] For massively inconsistent datasets (datasets with numerous contributors to inconsistency), these approaches can be overly

aggressive and result in excessive identifications. To address this challenge, Hegde and coworkers proposed *the vector consistency measure (VCM)* for resolving massively inconsistent datasets through the finding the fewest number of relaxations of the QoI lower and upper bounds required to render the dataset consistency.[16] Both strategies, SCM and VCM, are used in the present work for the data consistency analysis.

After a feasible set is constructed and dataset consistency is achieved, the reaction model optimization can be performed, e.g. through minimizing the sum of relative error between surrogate models and experimental data.[17] Generally, three scenarios of optimization are available in PrIMe. The first method applied is LS-$\mathcal{H}$, a (weighted) Least-Squared fit constraining parameter values to their initially assessed uncertainty ranges, $\mathcal{H}$. This is now quite common approach.[1-6,18] The other two refined methods,[17] LS-$\mathcal{F}$ and 1N-$\mathcal{F}$, are constrained to the posterior uncertainty ranges of parameters, over the feasible set $\mathcal{F}$. Method LS-$\mathcal{F}$ uses a weighted Least-Squared objective, while 1N-$\mathcal{F}$ is a 1-Norm minimization that aims at the smallest *number* of parameters to be changed.

In our recent research,[10] the initial H_2/CO reaction model, consisting of 73 reactions and 17 species, was subjected to a B2BDC analysis. A complete dataset including a total of 167 experimental targets (122 ignition delays, and 45 laminar flame speeds) and 55 active model parameters was constructed. Consistency analysis resulted in disagreement between model and data. Then, a final consistent dataset was composed by removing 45 experimental targets identified by VCM. Model optimization was performed with three methods, LS-$\mathcal{H}$, LS-$\mathcal{F}$ and 1N-$\mathcal{F}$. The LS-$\mathcal{F}$ model demonstrated the best agreement with experimental data resulting in zero number of the QoIs violation.

At the moment, it is unfortunately not guaranteed that a huge amount of data leads to a perfect well-predictive model, partly because the uncertainty prediction cannot be measured. In this work, we have augmented the dataset through a higher number of QoIs for syngas combustion by addition of more targets for already implemented[10] and newly published experimental observation sets. The selection criterion is the minimum amount of units sufficient to reflect the experimental trend. Moreover, a new dataset now covers the hydrogen ignition delay times and laminar flame speed measurements. The influence of this expansion on the consistency analysis, feasible set, and model optimization is analyzed and compared to the previous research results.

Performed consistency analysis has motivated us to investigate the results obtained with SCM and VCM methods and their comparison. Furthermore, the action regarding the inconsistent constraints identified by VCM analysis, either their elimination or bound relaxation, has been studied.

III. Workflow

A. Initial dataset

The construction of a dataset is one of the main requirements of the B2BDC methodology. A dataset must consist of the experimental observations with respective uncertainty bounds, and a common reaction kinetic model with active parameters identified via sensitivity analysis.[19]

In the initial dataset, syngas and hydrogen ignition delay times and laminar flame speeds are considered. For ignition delay times, a set of shock-tube ignition delay time measurements is selected. It has a wide range of temperatures (889-2136 K), pressures (0.6-33 bar), and equivalence ratios (φ=0.5-4). To account for flame-propagation conditions, a set of flame velocity measurements is selected for preheat temperatures (298-700 K), pressures (0.5-40 bar), and equivalence ratios (φ=0.5-5.6). These selected experimental observations cover the full range of operating conditions present in the literature sources. Experimental conditions of the selected measurements are summarized in Table 1. The uncertainty boundaries of the selected QoIs are assessed by evaluation with the empirical rule described in Slavinskaya et al.[10] The final number of QoIs in the complete is 477 QoIs, including 319 ignition delays and 158 laminar flame speeds. The selected QoIs of ignition delay times and laminar flame speeds along with their evaluated uncertainties can be found in Appendixes 1-2.

B. DLR_H_2/SynG reaction kinetic model

The chemical reaction kinetic model used in this research is a submodel of the DLR C_0-C_2 reaction model,[10] which is the base chemistry of the DLR reaction data base for larger hydrocarbon oxidation.

C. Ignition delay time determination

Ignition delay time might be derived from different indicators: pressure change, temperature or species concentration (usually OH* or OH). PrIMe allows the user to store experimental data with information about the

method used for ignition delay time determination. Nevertheless, the numerical simulation is not always able to identify uniquely the ignition delay time from OH* gradient raise.

Ignition delay time measurements					
Authors	Experimental conditions	Authors	Experimental conditions	Authors	Experimental conditions
Kalitan et al.[20]	T_5=900-1265 K; p_5=0.6-17.9 bar; ϕ=0.5	Mathieu et al.[21]	T_5=998-2012 K; p_5=1.6-32 atm; ϕ=0.5	Herzler and Naumann[22]	T_5=918-1238 K; p_5=1-16 atm; ϕ=0.5-1.0
Petersen et al.[23]	T_5=943-1148 K; p_5=16.50-32.7 bar; ϕ=0.5	Vasu et al.[24]	T_5=974-1160 K; p_5=1.3-2.5 bar; ϕ=0.5	Naumann et al.[25]	T_5=889-2136 K; p_5=1-16 atm; ϕ=0.1-4.0
Mertens et al.[26]	T_5=909-965 K; p_5=1.2-1.4 bar; ϕ=0.5-1.0	Thi et al.[27]	T_5=902.1-1268.7 K; p_5=2-20 atm; ϕ=1.0-1.5	Pan et al.[28]	T_5=915.1-1456.7 K; p_5=1.2 atm; ϕ=1.0
Mittal et al.[29]	T_5=1010.5-1044 K; p_5=15-50 bar; ϕ=1.0	Petersen et al.[30,31]	T_5=1189-1300 K; p_5=33 atm; ϕ=1.0	Zhang et al.[32]	T_5=1023.52-1267.23 K; p_5=5-20 atm; ϕ=0.5
Herzler and Naumann[33]	T_5=1019-1259K; p_5=14.0-16.91 bar; ϕ=0.5	Pang et al.[34]	T_5=906-1118 K; p_5=3.3-3.5 atm; ϕ=0.5	Slack[35]	T_5=986.62-1179.72 K; p_5=2 atm; ϕ=1.0
Krejci et al.[36]	T_5=980-2004 K; p_5=1.6-32.0 bar; ϕ=0.5				
Laminar flame speed measurements					
Sun et al.[37]	T_0=298 K; p=0.5-40.0 atm; ϕ=0.5-6.0	Goswami et al.[38]	T_0=298 K; p=1-10 atm; ϕ=0.5-0.6	Wang et al.[39]	T_0=298 K; p=1 atm; ϕ=0.6-5.6
Hassan et al.[40]	T_0=298 K; p=0.5-4.0 atm; ϕ=0.6-5.0	Zhang et al.[41]	T_0=298 K; p=1-10 atm; ϕ=0.5	Weng et al.[42]	T_0=295 K; p=1 atm; ϕ=0.6-2.0
Natarajan et al.[43]	T_0=300-700 K; p=1.0 atm; ϕ=0.59-1.01	Han et al.[44]	T_0=298 K; p=5-10 atm; ϕ=0.8	Xie et al.[45]	T_0=373 K; p=1-5 atm; ϕ=0.6-3.0
Natarajan et al.[46]	T_0=600 K; p=15 atm; ϕ=0.6-0.75	Lapalme and Seers[47]	T_0=295 K; p=1 atm; ϕ=0.6-2.2	Xie et al.[48]	T_0=373 K; p=1 atm; ϕ=0.6-3.0
Das et al.[49]	T_0=298-323 K; p=1.0 atm; ϕ=0.6-1.2	Li et al.[50]	T_0=295 K; p=1 atm; ϕ=0.6-1.0	Aung et al.[51] Taylor[52] Egolfopoulos and Law[53] Law[54] Vagelopoulos et al.[55] Hu et al.[56] Tang et al.[57] Verhelst et al.[58] Kwon and Faeth[59] Tse et al.[60]	T_0=298 K; p=1 atm; ϕ=0.5-4.5
Goswami et al.[61]	T_0=298 K; p=1-9 atm; ϕ=0.6-1.0	Sun et al.[62]	T_0=400 K; p=1 atm; ϕ=0.6-2.0	Tse et al.[60]	T_0=298 K; p=3-20 atm; ϕ=0.6-3.5

Table 1. Experimental measurements selected for initial dataset construction

It becomes more critical for ignition modeling of syngas, which has various ignition regimes: strong, mixed, and transient. This might cause the phenomena of an 'unclear' ignition event, for instance saddle point in the initial phase (Fig. 1a); the multi-peak behavior of OH* concentration profiles (Fig. 1b,c); peak s between the initial phase and steady state phase where the OH* concentration is constant in spite of ongoing processes (Fig. 1c); or absence of the gradient peaks. These behaviors are demonstrated in Fig. 1a-f. An ideal case of gradient raise is shown in Fig. 2.

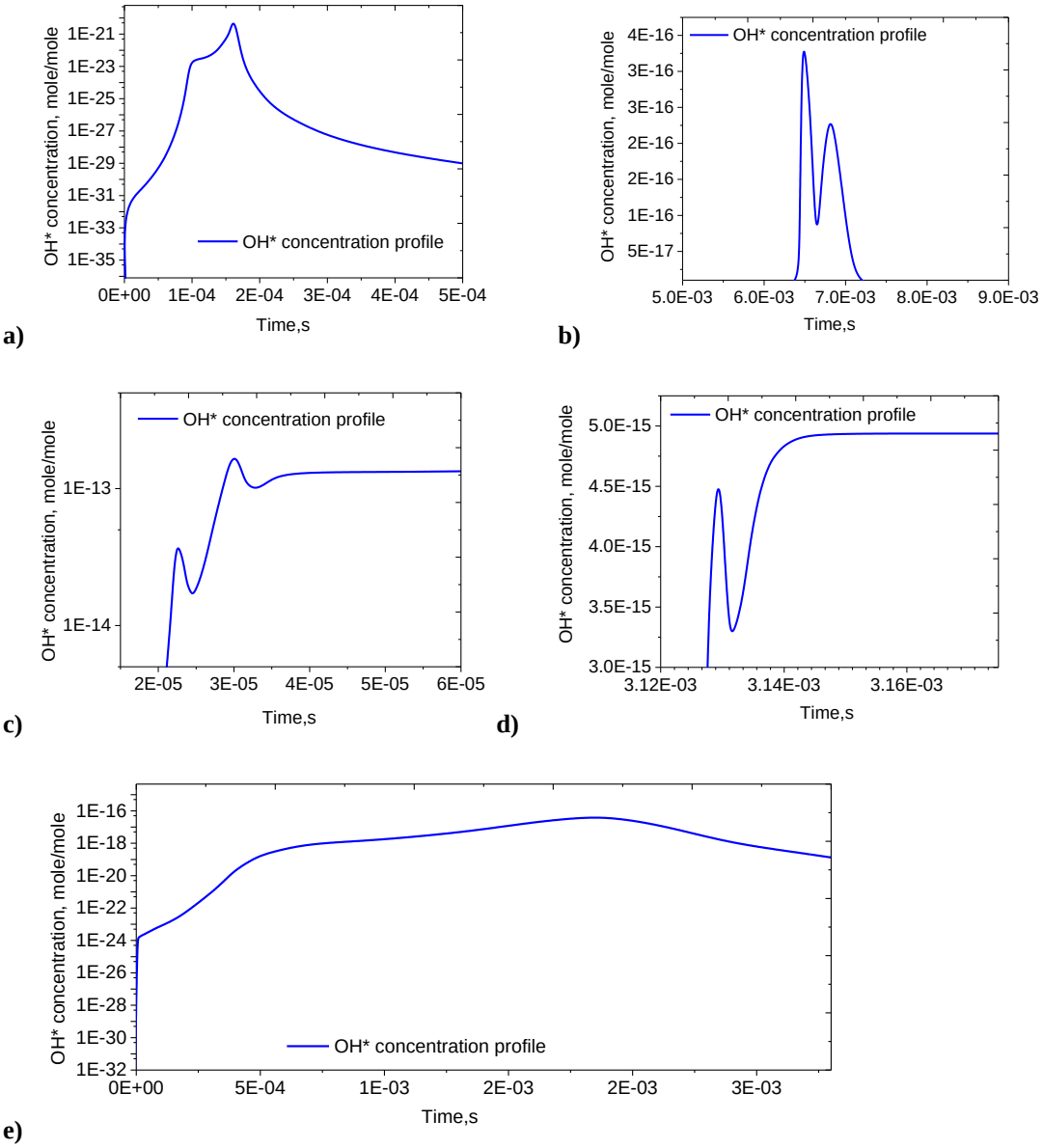

Figure 1. Different behaviors of OH* concentration profiles for ignition event determination

The misinterpretation of numerical results (selection of the 'false' peak as ignition time points) leads to the confuse conclusion about agreement/disagreement of surrogate model with experimental value and, as result, to erroneous feasible set and difficulties with data consistency analysis. To address this problem, the following assumptions have been made:

- When there are two peaks in the OH* profile as shown in Fig. 1a-c, the highest peak is used;

- When the simulated steady state OH* concentration is greater than the peak OH* concentration as shown in Fig. 1d, the peak OH* concentration is used;
- When there is no sharp gradient as shown in Fig. 1e, then the experimental point is assumed as self-inconsistent.

From the numerical point of view the OH* concentration profile does not seem to be a good indicator for syngas ignition determination. We have compared the step rise according to both pressure and temperature time histories along with the OH* concentration profile (Fig. 3a,b) for the QoI a00000238 with the initial model. It can be clearly seen that OH* concentration profile gives two peaks whereas very similar ignition delay time of 0.0123 s is obtained from both pressure and temperature profiles. This allows us to assume that all three indicators for ignition time determination interchangeable and recommend using pressure and/or temperature profile as a unique indicator of ignition delay time for all QoIs.

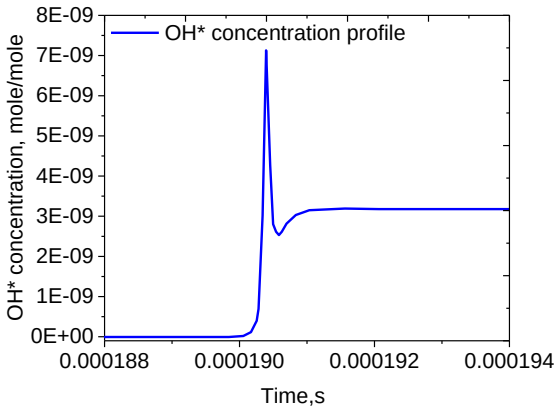

Figure 2. 'Ideal' case of OH* concentration profile for ignition event determination

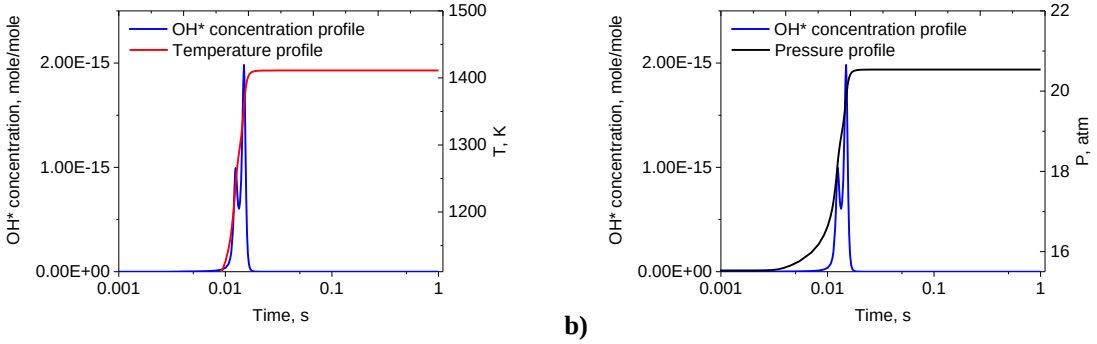

Figure 3. Comparison of different indicators for ignition time determination

D. Preliminary filtering

In order to provide more accurate fitting, a preliminary filtering is applied on the QoIs. According to the filtering results, eleven QoIs, a00000156, a00000157, a00000158, a00000309, a00000352, a00000355, a00000358, a00000359, a00000360, a00000701, and a00000504 (according to the case explained in Fig. 1e) are detected as self-inconsistent and removed before any further analysis. We assume that some of those QoIs stem from large deviation of modeled ignition time from the experimentally observed one, and some, perhaps, from the large ranges of parameter uncertainties.

E. Construction of feasible region F

The change in prior (original domain $\mathcal{H}$) and posterior (feasible set $\mathcal{F}$) parameter bounds for DLR_H_2/SynG dataset is demonstrated in Fig. 4. The variable index indicates the active model parameters. The full list of active parameters and their uncertainty bounds of rate coefficients is given in Slavinskaya et al.[10] Uncertainty bounds are given as a relative value. Also shown, as black vertical lines, are prior parameter uncertainty bounds, whereas blue and red lines are the posterior inner and outer bounds, respectively.

F. Consistency analysis

After applying the preliminary filtration, a new dataset is generated after removing 11 self-inconsistent QoIs via preliminary filtering. This dataset, which includes 466 total QoIs, is originally inconsistent. After performing SCM analysis, the SCM interval γ (Eq. 3) for the original dataset is found to be [-2.51, -2.31]. Since the SCM value is negative, the dataset is inconsistent.

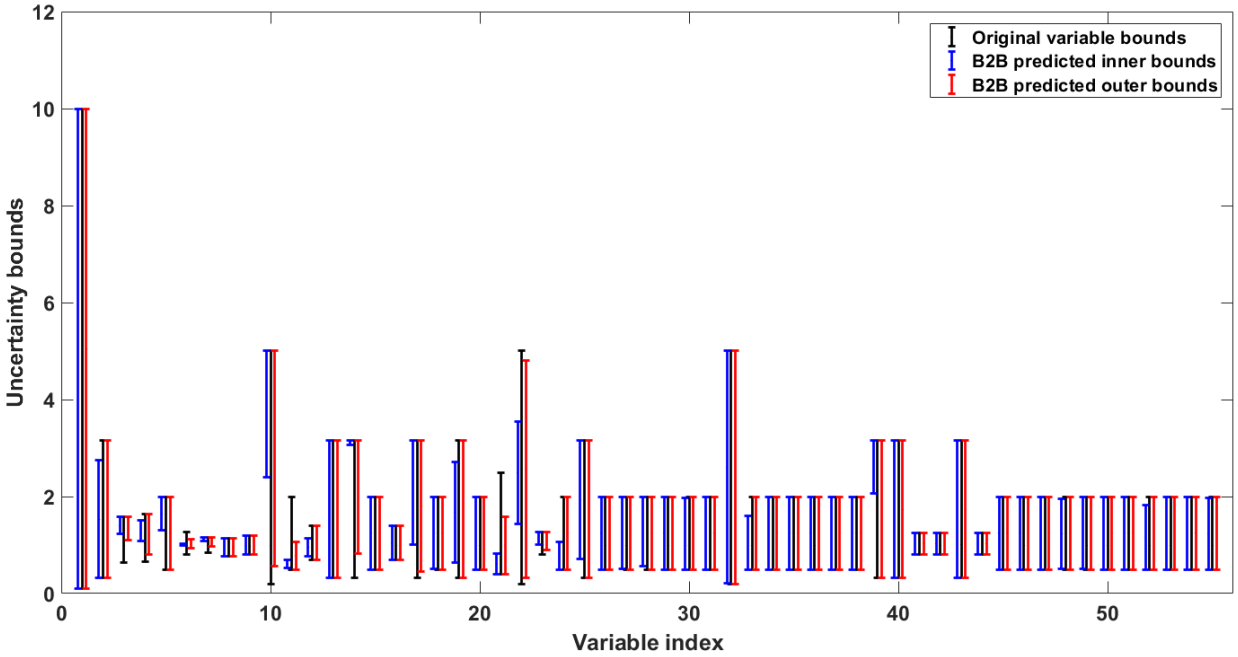

Figure 4. Prior and posterior parameter bounds

VCM analysis results in 87 targets to be relaxed or removed by VCM. These 87 QoIs consisting of 84 ignition delay QoIs and 3 flame speed QoIs are presented in Appendix 3. However, after the detailed analysis of all 87 QoIs, it has to be noted that this amount is overestimated, and mathematical algorithm still should be further investigated and improved. 87 QoIs are removed resulting in DLR_H_2/SynG dataset with SCM interval γ equal to [0.047, 0.11]. The SCM is now positive, thus the final DLR_H_2/SynG dataset containing 379 QoIs is consistent.

G. Parameter optimization and validation with experimental data

Parameter optimization is designed to find an optimal point in the parameter space minimizing specified objectives. Generally, three types of optimization were applied:

1. LS-$\mathcal{F}$ – minimizing the sum of relative error between surrogate models and experimental data over the feasible set.
2. LS-$\mathcal{H}$ – minimizing the sum of relative error between surrogate models and experimental data over the original domain.
3. 1N-$\mathcal{F}$ – minimizing the 1-norm of the parameter over the feasible set.

The data presented in Table 2 show a similar trend as in the previous research[10] and highlight several features. According to the obtained results the lowest average deviation is shown by LS-$\mathcal{H}$ optimization. It was constrained to the prior uncertainty ranges of parameters, over the original domain $\mathcal{H}$. Nevertheless, LS-$\mathcal{H}$ results in violation of 28 QoIs uncertainty bounds. At the same time, the LS-$\mathcal{F}$ and 1N-$\mathcal{F}$ optimization methods, constrained to the posterior uncertainty ranges of parameters, over the feasible set $\mathcal{F}$, result in a lower average relative error and zero number of QoIs violation. The 1N-$\mathcal{F}$ scheme is using the least number of parameter changes, minimizing the 1-norm of the parameter; therefore, it gives higher error as compared to the LS-$\mathcal{F}$. Thus, we can conclude that LS-$\mathcal{F}$ optimization method demonstrates the best predicting behavior among the three methods and will be used in the current study.

Optimization method	Average error (%)	Number of QoIs violations
LS-$\mathcal{F}$	24.4	0
LS-$\mathcal{H}$	21.7	28
1N-$\mathcal{F}$	40.6	0

Table 2. Comparison of the optimization methods based on the surrogate models, pw

A comparison between initial and final optimized model validated on experimental data is presented in Figures 5-6. Model predictions are also compared with those of Varga et al.[6] since it was generated on the similar optimization method with much bigger amount of QoIs but without mathematical analysis of data consistency.

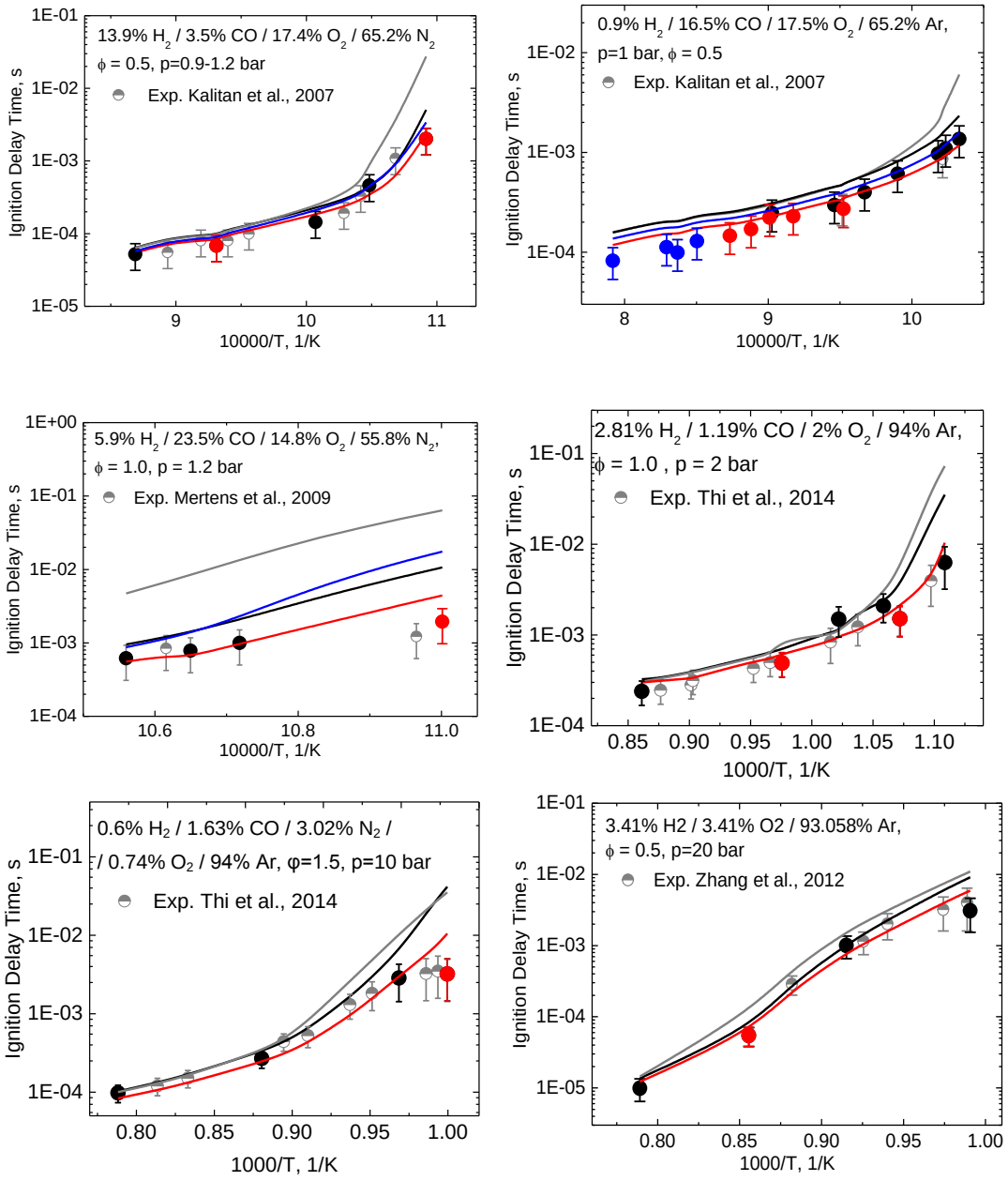

Figure 5. Syngas and hydrogen ignition delay time simulations. *Symbols, experimental data; initial DLR model, black line; Varga et al. model,[6] gray solid line; LS-$\mathcal{F}$ optimized model, pw, red solid line; LS-$\mathcal{F}$ optimized model,[10] blue solid line; Black full circles are QoIs from DLR_H2/SynG dataset; Red full circles are the QoIs deleted from the initial dataset according to the VCM analysis; Blue full circles are the self-inconsistent QoIs deleted from the initial dataset before any analysis.*

Comparisons in Fig. 5 demonstrate that the predictions of the optimized model overall are in good agreement with the experimental measurements obtained in shock tubes. Fig. 6 shows the validation of initial and optimized models on the laminar flame speed data. The LS-$\mathcal{F}$ optimization method significantly improves model prediction accuracy against experimental results over low temperature regime of most significance in modeling ignition delay

times. However, for some QoIs, there is no visible influence of the model optimization. Overall, the LS-$\mathcal{F}$ optimized model predicts the experimental data within the experimental uncertainties in case of consistent QoIs excluding those removed after VCM analysis (red circles with cross).

The results also demonstrate the influence of dataset augmentation. The comparison of LS-$\mathcal{F}$ models prediction applied on the dataset with total 122 QoIs[10] and 379 QoIs (pw) clearly indicates several points:

- From each experimental set, there should be sufficient amount of experimental points to reproduce the trend;
- Since the investigated reaction mechanism covers hydrogen and syngas combustion, construction of heterogeneous dataset (QoIs of both hydrogen and syngas) results in a higher confidence level of the model uncertainty quantification and, in consequence, better predictions of the optimized model.

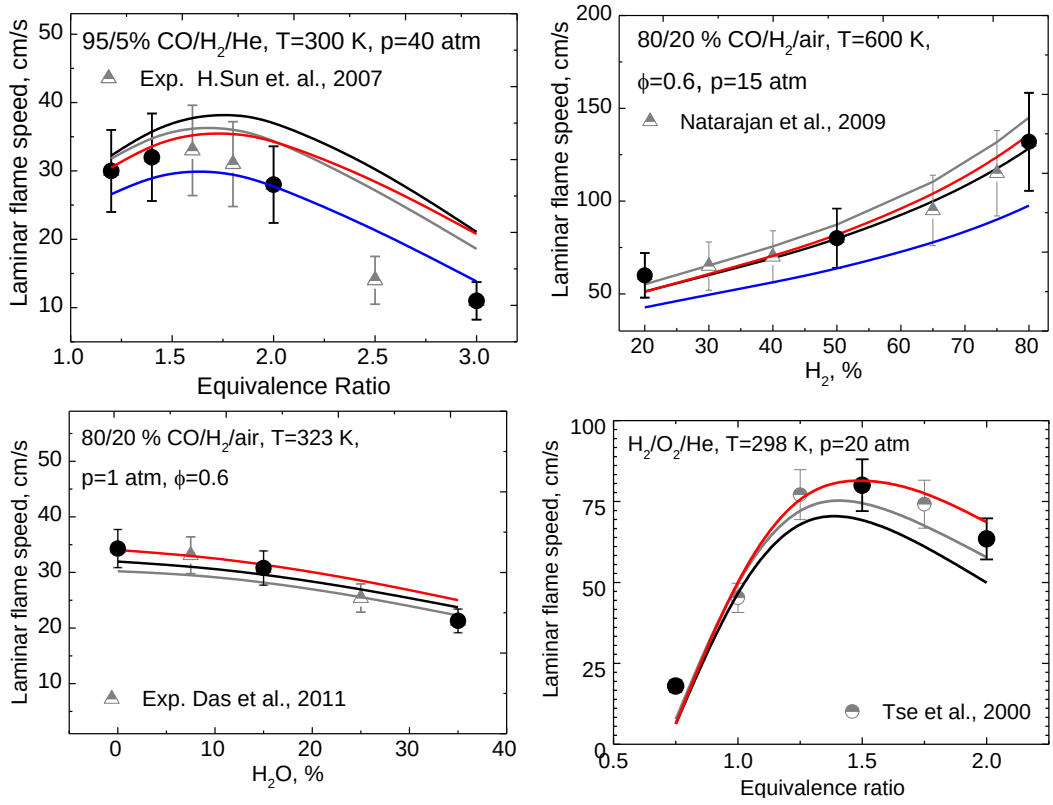

Figure 6. Syngas and hydrogen laminar flame speed simulations. *Symbols, experimental data; initial DLR model, black line; Varga et al. model,[6] gray solid line; LS-$\mathcal{F}$ optimized model, pw, red solid line; LS-$\mathcal{F}$ optimized model,[10] blue solid line; Black full circles are QoIs from DLR_H2/SynG dataset.*

IV. Conclusion

In this paper, B2BDC analysis of large amount of hydrogen and syngas combustion data was applied within the PrIMe cyber-infrastructure for investigation of dataset construction parameters and their impact on reaction model optimization.

The detailed syngas oxidation mechanism of Slavinskaya et al.[10] has been updated using recently published rate constants. The approach of combined SCM and VCM methods for consistency analysis has been adapted from Hegde et al.[16] and successfully implemented.

The problem of ignition delay determination based on OH* concentration profile has been discussed and clarified. According to the research analysis, it has been recommended to use temperature and/or pressure time histories as a unique criterion of syngas ignition delay times for numerical simulations in PrIMe.

Dataset augmentation was performed and investigated. It has been found out that dataset augmentation has resulted in better prediction behavior of optimized model.

Finally, predictions using the present LS-$\mathcal{F}$ optimized mechanism were compared against a wide range of experimental data of laminar premixed flames and shock tube ignition delay times. Improvement of optimized model prediction results can be clearly seen. Good agreement of model predictions with the experimental measurements allows us to further develop a complex uncertainty quantified H_2-CO model for hydrogen and syngas combustion.

Appendix

Appendix 1. Ignition delay time QoIs

#	Mixture	T_5, K	P_5, bar	Attribute ID	Estimated error, %	#	Mixture	T, K	p, bar	Attribute ID	Estimated error, %
1	40/60%CO/H2/air	914.0	1.1	a00000105	20	162	2.81%H2/1.19%CO/2%O2/94%Ar	1089.3	9.3	a00000558	25
2	40/60%CO/H2/air	1036.0	1.1	a00000106	20	163	2.81%H2/1.19%CO/2%O2/94%Ar	1061.5	9.2	a00000559	35
3	40/60%CO/H2/air	1241.0	1.0	a00000107	20	164	2.81%H2/1.19%CO/2%O2/94%Ar	1020.5	10.0	a00000560	50
4	60/40%CO/H2/air	900.0	0.6	a00000110	20	165	2.81%H2/1.19%CO/2%O2/94%Ar	937.7	9.5	a00000561	60
5	60/40%CO/H2/air	1026.0	1.1	a00000111	20	166	2.81%H2/1.19%CO/2%O2/94%Ar	1182.9	19.5	a00000562	30
6	60/40%CO/H2/air	1162.0	1.0	a00000112	20	167	2.81%H2/1.19%CO/2%O2/94%Ar	1097.1	20.3	a00000563	35
7	3.5%H2/14%CO/17.4%O2/65.1%Ar	936.0	1.2	a00000113	20	168	2.81%H2/1.19%CO/2%O2/94%Ar	1039.1	20.0	a00000564	50
8	3.5%H2/14%CO/17.4%O2/65.1%Ar	1058.0	2.6	a00000114	20	169	2.81%H2/1.19%CO/2%O2/94%Ar	1035.3	20.4	a00000565	60
9	3.5%H2/14%CO/17.4%O2/65.1%Ar	1190.0	16.8	a00000115	20	170	2.81%H2/1.19%CO/2%O2/94%Ar	1024.4	17.2	a00000566	75
10	1.7%H2/15.6%CO/17.5%O2/65.2% Ar	960.0	1.2	a00000116	20	171	1.5%H2/3.0%CO/1.5%O2/94%Ar	1227.3	1.7	a00000567	25
11	1.7%H2/15.6%CO/17.5%O2/65.2% Ar	1118.0	2.5	a00000117	20	172	1.5%H2/3.0%CO/1.5%O2/94%Ar	1053.3	1.9	a00000568	35
12	1.7%H2/15.6%CO/17.5%O2/65.2% Ar	1265.0	17.1	a00000118	20	173	1.5%H2/3.0%CO/1.5%O2/94%Ar	945.1	1.8	a00000569	45
13	0.9%H2/16.5%CO/17.5%O2/65.2% Ar	1121.0	14.0	a00000121	20	174	1.5%H2/3.0%CO/1.5%O2/94%Ar	898.4	1.9	a00000570	80
14	40/60%CO/H2/air	951.0	1.1	a00000131	20	175	1.5%H2/3.0%CO/1.5%O2/94%Ar	1221.4	10.0	a00000571	25
15	40/60%CO/H2/air	996.0	1.1	a00000132	20	176	1.5%H2/3.0%CO/1.5%O2/94%Ar	1070.4	9.7	a00000572	30
16	40/60%CO/H2/air	1072.0	1.1	a00000133	20	177	1.5%H2/3.0%CO/1.5%O2/94%Ar	1010.4	9.6	a00000573	55
17	40/60%CO/H2/air	1125.0	1.1	a00000134	20	178	1.5%H2/3.0%CO/1.5%O2/94%Ar	1247.3	21.1	a00000574	35
18	40/60%CO/H2/air	1175.0	1.0	a00000135	20	179	1.5%H2/3.0%CO/1.5%O2/94%Ar	1133.0	19.9	a00000575	30
19	40/60%CO/H2/air	1187.0	1.0	a00000136	20	180	1.5%H2/3.0%CO/1.5%O2/94%Ar	1046.0	20.2	a00000576	60
20	0.9%H2/16.5%CO/17.5%O2/65.2% Ar	977.0	1.2	a00000146	20	181	1.54%H2/1.57%CO/1.34%CO2/1.55%O2/94%Ar	1200.0	1.8	a00000577	25
21	0.9%H2/16.5%CO/17.5%O2/65.2% Ar	982.0	1.1	a00000147	20	182	1.54%H2/1.57%CO/1.34%CO2/1.55%O2/94%Ar	1064.1	1.8	a00000578	30
22	0.9%H2/16.5%CO/17.5%O2/65.2% Ar	1010.0	1.2	a00000148	20	183	1.54%H2/1.57%CO/1.34%CO2/1.55%O2/94%Ar	958.5	1.9	a00000579	45
23	0.9%H2/16.5%CO/17.5%O2/65.2% Ar	1034.0	1.1	a00000149	20	184	1.54%H2/1.57%CO/1.34%CO2/1.55%O2/94%Ar	915.6	1.9	a00000580	60
24	0.9%H2/16.5%CO/17.5%O2/65.2% Ar	1050.0	1.1	a00000150	20	185	1.54%H2/1.57%CO/1.34%CO2/1.55%O2/94%Ar	1257.6	9.8	a00000581	25
25	0.9%H2/16.5%CO/17.5%O2/65.2% Ar	1108.0	1.1	a00000151	20	186	1.54%H2/1.57%CO/1.34%CO2/1.55%O2/94%Ar	1101.9	9.6	a00000582	30
26	0.9%H2/16.5%CO/17.5%O2/65.2% Ar	1090.0	1.1	a00000152	20	187	1.54%H2/1.57%CO/1.34%CO2/1.55%O2/94%Ar	1055.7	9.8	a00000583	35
27	0.9%H2/16.5%CO/17.5%O2/65.2% Ar	1110.0	1.1	a00000153	20	188	1.54%H2/1.57%CO/1.34%CO2/1.55%O2/94%Ar	1036.2	8.2	a00000584	40
28	0.9%H2/16.5%CO/17.5%O2/65.2% Ar	1126.0	1.1	a00000154	20	189	1.54%H2/1.57%CO/1.34%CO2/1.55%O2/94%Ar	1026.8	10.2	a00000585	55
29	0.9%H2/16.5%CO/17.5%O2/65.2% Ar	1145.0	1.1	a00000155	20	190	1.54%H2/1.57%CO/1.34%CO2/1.55%O2/94%Ar	1015.6	10.1	a00000586	50
30	0.9%H2/16.5%CO/17.5%O2/65.2% Ar	1176.0	1.0	a00000156	20	191	1.54%H2/1.57%CO/1.34%CO2/1.55%O2/94%Ar	1238.6	20.2	a00000587	35
31	0.9%H2/16.5%CO/17.5%O2/65.2% Ar	1195.0	1.1	a00000157	20	192	1.54%H2/1.57%CO/1.34%CO2/1.55%O2/94%Ar	1151.3	20.0	a00000588	30
32	0.9%H2/16.5%CO/17.5%O2/65.2% Ar	1206.0	1.0	a00000158	20	193	1.54%H2/1.57%CO/1.34%CO2/1.55%O2/94%Ar	1103.7	20.2	a00000589	40
33	0.9%H2/16.5%CO/17.5%O2/65.2% Ar	1005.0	2.3	a00000159	20	194	1.54%H2/1.57%CO/1.34%CO2/1.55%O2/94%Ar	1051.0	19.3	a00000590	55
34	20/80%CO/H2/air	916.0	1.1	a00000179	20	195	0.6%H2/1.63%CO/3.02%N2/0.74%O2/94%Ar	1175.8	1.9	a00000591	25
35	20/80%CO/H2/air	954.0	1.2	a00000181	20	196	0.6%H2/1.63%CO/3.02%N2/0.74%O2/94%Ar	1039.4	1.9	a00000592	35
36	20/80%CO/H2/air	993.0	1.0	a00000183	20	197	0.6%H2/1.63%CO/3.02%N2/0.74%O2/94%Ar	964.2	1.8	a00000593	50
37	20/80%CO/H2/air	1074.0	1.1	a00000186	20	198	0.6%H2/1.63%CO/3.02%N2/0.74%O2/94%Ar	943.5	2.0	a00000594	55
38	20/80%CO/H2/air	1151.0	1.0	a00000188	20	199	0.6%H2/1.63%CO/3.02%N2/0.74%O2/94%Ar	939.6	1.9	a00000595	55
39	3.5%H2/14%CO/17.4%O2/65.1%Ar	1015.0	1.1	a00000189	20	200	0.6%H2/1.63%CO/3.02%N2/0.74%O2/94%Ar	940.2	2.0	a00000596	70
40	3.5%H2/14%CO/17.4%O2/65.1%Ar	1183.0	1.1	a00000190	20	201	0.6%H2/1.63%CO/3.02%N2/0.74%O2/94%Ar	1268.7	10.2	a00000597	25
41	3.5%H2/14%CO/17.4%O2/65.1%Ar	929.0	2.6	a00000191	20	202	0.6%H2/1.63%CO/3.02%N2/0.74%O2/94%Ar	1135.8	9.3	a00000598	25
42	3.5%H2/14%CO/17.4%O2/65.1%Ar	992.0	2.6	a00000192	20	203	0.6%H2/1.63%CO/3.02%N2/0.74%O2/94%Ar	1032.5	10.3	a00000599	50

#	Mixture	T_5, K	P_5, bar	Attribute ID	Estimated error, %	#	Mixture	T, K	p, bar	Attribute ID	Estimated error, %
43	3.5%H2/14%CO/17.4%O2/65.1%Ar	1063.0	3.1	a00000193	20	204	0.6%H2/1.63%CO/3.02%N2/0.74%O2/94%Ar	1000.4	10.1	a00000600	55
44	3.5%H2/14%CO/17.4%O2/65.1%Ar	1114.0	14.9	a00000194	20	205	0.6%H2/1.63%CO/3.02%N2/0.74%O2/94%Ar	1226.9	19.7	a00000601	25
45	1.7%H2/15.6%CO/17.5%O2/65.2%Ar	1052.0	1.1	a00000195	20	206	0.6%H2/1.63%CO/3.02%N2/0.74%O2/94%Ar	1174.7	20.2	a00000602	25
46	1.7%H2/15.6%CO/17.5%O2/65.2%Ar	1197.0	1.1	a00000196	20	207	0.6%H2/1.63%CO/3.02%N2/0.74%O2/94%Ar	1133.9	20.0	a00000603	30
47	1.7%H2/15.6%CO/17.5%O2/65.2%Ar	981.0	2.7	a00000197	20	208	0.6%H2/1.63%CO/3.02%N2/0.74%O2/94%Ar	1104.3	20.5	a00000604	40
48	1.7%H2/15.6%CO/17.5%O2/65.2%Ar	1048.0	2.5	a00000198	20	209	0.6%H2/1.63%CO/3.02%N2/0.74%O2/94%Ar	1100.1	19.7	a00000605	30
49	1.7%H2/15.6%CO/17.5%O2/65.2%Ar	1063.0	14.3	a00000199	20	210	0.6%H2/1.63%CO/3.02%N2/0.74%O2/94%Ar	1098.1	20.9	a00000606	45
50	1.7%H2/15.6%CO/17.5%O2/65.2%Ar	1126.0	11.9	a00000200	20	211	0.6%H2/1.63%CO/3.02%N2/0.74%O2/94%Ar	1073.2	20.3	a00000607	50
51	0.9%H2/16.5%CO/17.5%O2/65.2%Ar	1114.0	2.1	a00000203	20	212	2%H2/1%O2/97%Ar	1300.0	33.0	a00000608	45
52	0.9%H2/16.5%CO/17.5%O2/65.2%Ar	1074.0	19.2	a00000205	20	213	2%H2/1%O2/97%Ar	1264.0	33.0	a00000609	45
53	0.9%H2/16.5%CO/17.5%O2/65.2%Ar	1114.0	14.6	a00000206	20	214	2%H2/1%O2/97%Ar	1221.0	33.0	a00000610	40
54	7.33%H2/9.71%CO/1.98%CO2/17.01%O2/63.97%N2	1013.0	21.6	a00000208	20	215	2%H2/1%O2/97%Ar	1189.0	33.0	a00000611	40
55	0.5%H2/14%CO/17.4%O2/65.1%Ar	1015.0	13.7	a00000213	20	216	4%H2/2%O2/94%Ar	930.0	3.6	a00000612	45
56	80/20%CO/H2/air	939.0	1.1	a00000221	30	217	4%H2/2%O2/94%Ar	938.0	3.5	a00000613	40
57	15.6%CO/1.7%H2/17.5%O2/65.2%Ar	932.0	1.4	a00000223	30	218	4%H2/2%O2/94%Ar	964.0	3.6	a00000614	35
58	15.6%CO/1.7%H2/17.5%O2/65.2%Ar	956.0	1.4	a00000224	30	219	4%H2/2%O2/94%Ar	987.0	3.4	a00000615	30
59	15.6%CO/1.7%H2/17.5%O2/65.2%Ar	965.0	1.5	a00000225	30	220	4%H2/2%O2/94%Ar	1021.0	3.4	a00000616	20
60	0.436%H2/8.228%CO/8.657%O2/82.679%Ar	1046.0	16.8	a00000226	20	221	4%H2/2%O2/94%Ar	1118.0	3.4	a00000617	20
61	0.436%H2/8.228%CO/8.657%O2/82.679%Ar	1072.0	15.8	a00000227	20	222	15%H2/18%O2/67%Ar	908.0	3.4	a00000618	40
62	0.436%H2/8.228%CO/8.657%O2/82.679%Ar	1132.0	16.2	a00000228	20	223	15%H2/18%O2/67%Ar	919.0	3.4	a00000619	40
63	0.175%H2/3.301%CO/3.473%O2/93.051%Ar	1107.0	16.2	a00000229	20	224	15%H2/18%O2/67%Ar	951.0	3.3	a00000620	30
64	0.175%H2/3.301%CO/3.473%O2/93.051%Ar	1159.0	16.1	a00000230	20	225	15%H2/18%O2/67%Ar	992.0	3.2	a00000621	25
65	0.175%H2/3.301%CO/3.473%O2/93.051%Ar	1206.0	16.4	a00000231	20	226	15%H2/18%O2/67%Ar	1049.0	3.0	a00000622	25
66	0.088%H2/1.654%CO/1.740%O2/96.518Ar	1165.0	16.1	a00000232	20	227	3.46%H2/3.49%O2/93.05%Ar	923.0	1.0	a00000623	35
67	0.088%H2/1.654%CO/1.740%O2/96.518Ar	1207.0	16.4	a00000233	20	228	3.46%H2/3.49%O2/93.05%Ar	934.0	1.1	a00000624	35
68	0.088%H2/1.654%CO/1.740%O2/96.518Ar	1259.0	15.9	a00000234	20	229	3.46%H2/3.49%O2/93.05%Ar	941.0	1.1	a00000625	30
69	4.364%H2/4.364%CO/8.718%O2/82.554%Ar	1019.0	14.1	a00000235	20	230	3.46%H2/3.49%O2/93.05%Ar	1027.0	1.0	a00000626	20
70	4.364%H2/4.364%CO/8.718%O2/82.554%Ar	1051.0	15.3	a00000236	20	231	5.87%H2/2.95%O2/91.18%Ar	918.0	1.0	a00000627	35
71	4.364%H2/4.364%CO/8.718%O2/82.554%Ar	1097.0	15.6	a00000237	20	232	5.87%H2/2.95%O2/91.18%Ar	956.0	0.9	a00000628	30
72	1.77%H2/1.80%CO/3.559%O2/92.87%Ar	1048.0	16.0	a00000238	20	233	5.87%H2/2.95%O2/91.18%Ar	1061.0	1.0	a00000629	20
73	1.77%H2/1.80%CO/3.559%O2/92.87%Ar	1086.0	15.5	a00000239	20	234	5.87%H2/2.95%O2/91.18%Ar	1718.0	1.1	a00000630	30
74	1.77%H2/1.80%CO/3.559%O2/92.87%Ar	1128.0	15.5	a00000240	20	235	3.46%H2/3.49%O2/93.05%Ar	958.0	3.9	a00000631	35
75	0.868%H2/0.868%CO/1.736%O2/96.529%Ar	1054.0	15.6	a00000241	20	236	3.46%H2/3.49%O2/93.05%Ar	992.0	4.0	a00000632	30
76	0.868%H2/0.868%CO/1.736%O2/96.529%Ar	1090.0	15.8	a00000242	20	237	3.46%H2/3.49%O2/93.05%Ar	1035.0	3.8	a00000633	20
77	0.868%H2/0.868%CO/1.736%O2/96.529%Ar	1140.0	15.9	a00000243	20	238	5.87%H2/2.95%O2/91.18%Ar	964.0	4.1	a00000634	35
78	60/40%CO/H2/air	1169.0	1.0	a00000286	20	239	5.87%H2/2.95%O2/91.18%Ar	1002.0	4.0	a00000635	25
79	1.7%H2/15.6%CO/17.5%O2/65.2%Ar	1033.0	1.1	a00000299	20	240	5.87%H2/2.95%O2/91.18%Ar	1051.0	4.0	a00000636	20
80	1.7%H2/15.6%CO/17.5%O2/65.2%Ar	991.0	2.6	a00000301	20	241	5.87%H2/2.95%O2/91.18%Ar	1160.0	4.1	a00000637	20
81	1.7%H2/15.6%CO/17.5%O2/65.2%Ar	1060.0	2.1	a00000302	20	242	3.46%H2/3.49%O2/93.05%Ar	1018.0	15.4	a00000638	35
82	1.7%H2/15.6%CO/17.5%O2/65.2%Ar	1148.0	2.3	a00000303	20	243	3.46%H2/3.49%O2/93.05%Ar	1068.0	16.1	a00000639	30
83	1.7%H2/15.6%CO/17.5%O2/65.2%Ar	1090.0	13.6	a00000304	20	244	3.46%H2/3.49%O2/93.05%Ar	1109.0	16.0	a00000640	25
84	1.7%H2/15.6%CO/17.5%O2/65.2%Ar	1158.0	14.7	a00000305	20	245	3.46%H2/3.49%O2/93.05%Ar	1121.0	15.1	a00000641	25

#	Mixture	T_5, K	P_5, bar	Attribute ID	Estimated error, %	#	Mixture	T, K	p, bar	Attribute ID	Estimated error, %
85	0.9%H2/16.5%CO/17.5%O2/65.2% Ar	968.0	1.2	a00000307	20	246	5.87%H2/2.95%O2/91.18%Ar	1015.0	15.1	a00000642	35
86	0.9%H2/16.5%CO/17.5%O2/65.2% Ar	1057.0	1.1	a00000308	20	247	5.87%H2/2.95%O2/91.18%Ar	1098.0	15.1	a00000643	25
87	0.9%H2/16.5%CO/17.5%O2/65.2% Ar	1263.0	1.1	a00000309	20	248	5.87%H2/2.95%O2/91.18%Ar	1207.0	17.4	a00000644	30
88	0.9%H2/16.5%CO/17.5%O2/65.2% Ar	977.0	2.3	a00000310	20	249	5.87%H2/2.95%O2/91.18%Ar	1238.0	19.3	a00000645	30
89	0.9%H2/16.5%CO/17.5%O2/65.2% Ar	1149.0	2.0	a00000311	20	250	3.47%H2/3.47%O2/93.06%N2	932.0	0.9	a00000646	40
90	0.9%H2/16.5%CO/17.5%O2/65.2% Ar	1304.0	1.7	a00000312	20	251	3.47%H2/3.47%O2/93.06%N2	968.0	1.0	a00000647	30
91	0.9%H2/16.5%CO/17.5%O2/65.2% Ar	1110.0	12.7	a00000313	20	252	3.47%H2/3.47%O2/93.06%N2	992.0	1.0	a00000648	30
92	7.33%H2/9.71%CO/1.98%CO2/17.01%O2/63.97%N2	943.0	22.3	a00000316	20	253	3.47%H2/3.47%O2/93.06%N2	1954.0	1.0	a00000649	25
93	7.33%H2/9.71%CO/1.98%CO2/17.01%O2/63.97%N2	1033.0	23.7	a00000317	20	254	0.81%H2/4.03%O2/95.16%Ar	939.0	1.0	a00000650	40
94	7.33%H2/9.71%CO/1.98%CO2/17.01%O2/63.97%N2	1148.0	21.4	a00000318	20	255	0.81%H2/4.03%O2/95.16%Ar	1026.0	1.0	a00000651	25
95	80/20%CO/H2/air	909.0	1.2	a00000322	30	256	0.81%H2/4.03%O2/95.16%Ar	1267.0	0.8	a00000652	20
96	80/20%CO/H2/air	933.0	1.2	a00000323	30	257	0.81%H2/4.03%O2/95.16%Ar	1670.0	0.9	a00000653	25
97	80/20%CO/H2/air	947.0	1.2	a00000324	30	258	0.81%H2/4.03%O2/95.16%Ar	2109.0	1.1	a00000654	30
98	0.8%H2/0.2%CO/1%O2/98%Ar	1299.0	12.0	a00000334	20	259	4.03%H2/20.16%O2/75.81%Ar	889.0	1.0	a00000655	35
99	0.8%H2/0.2%CO/1%O2/98%Ar	1182.0	12.0	a00000335	20	260	4.03%H2/20.16%O2/75.81%Ar	897.0	1.1	a00000656	35
100	0.8%H2/0.2%CO/1%O2/98%Ar	1096.0	12.0	a00000336	20	261	4.03%H2/20.16%O2/75.81%Ar	975.0	1.1	a00000657	25
101	0.5%H2/0.5%CO/1%O2/98%Ar	1383.0	12.0	a00000337	20	262	4.03%H2/20.16%O2/75.81%Ar	1154.0	0.7	a00000658	20
102	0.5%H2/0.5%CO/1%O2/98%Ar	1235.0	12.0	a00000338	20	263	4.03%H2/20.16%O2/75.81%Ar	1675.0	1.1	a00000659	30
103	0.5%H2/0.5%CO/1%O2/98%Ar	1099.0	12.0	a00000339	20	264	12.54%H2/1.57%O2/85.89%Ar	943.0	1.1	a00000660	35
104	0.1%H2/0.9%CO/1%O2/98%Ar	1387.0	12.0	a00000340	20	265	12.54%H2/1.57%O2/85.89%Ar	953.0	0.9	a00000661	30
105	0.1%H2/0.9%CO/1%O2/98%Ar	1228.0	12.0	a00000341	20	266	12.54%H2/1.57%O2/85.89%Ar	976.0	1.1	a00000662	30
106	0.1%H2/0.9%CO/1%O2/98%Ar	1116.0	12.0	a00000342	20	267	12.54%H2/1.57%O2/85.89%Ar	1074.0	1.1	a00000663	25
107	0.8%H2/0.2%CO/1%O2/98%Ar	1264.0	32.0	a00000343	20	268	12.54%H2/1.57%O2/85.89%Ar	1288.0	0.9	a00000664	20
108	0.8%H2/0.2%CO/1%O2/98%Ar	1243.0	32.0	a00000344	20	269	12.54%H2/1.57%O2/85.89%Ar	2136.0	1.4	a00000665	30
109	0.8%H2/0.2%CO/1%O2/98%Ar	1185.0	32.0	a00000345	20	270	3.47%H2/3.47%O2/93.06%N2	1006.0	3.9	a00000666	30
110	0.5%H2/0.5%CO/1%O2/98%Ar	1325.0	32.0	a00000346	20	271	3.47%H2/3.47%O2/93.06%N2	1037.0	4.1	a00000667	25
111	0.5%H2/0.5%CO/1%O2/98%Ar	1204.0	32.0	a00000347	20	272	3.47%H2/3.47%O2/93.06%N2	1060.0	4.2	a00000668	25
112	0.5%H2/0.5%CO/1%O2/98%Ar	1179.0	32.0	a00000348	20	273	3.47%H2/3.47%O2/93.06%N2	1081.0	3.9	a00000669	20
113	0.1%H2/0.9%CO/1%O2/98%Ar	1327.0	32.0	a00000349	20	274	3.47%H2/3.47%O2/93.06%N2	1257.0	3.9	a00000670	20
114	0.1%H2/0.9%CO/1%O2/98%Ar	1259.0	32.0	a00000350	20	275	0.81%H2/4.03%O2/95.16%Ar	935.0	3.9	a00000671	40
115	0.1%H2/0.9%CO/1%O2/98%Ar	1166.0	32.0	a00000351	20	276	0.81%H2/4.03%O2/95.16%Ar	986.0	3.9	a00000672	30
116	0.8%H2/0.2%CO/1%O2/98%Ar	1695.0	1.6	a00000352	20	277	0.81%H2/4.03%O2/95.16%Ar	1075.0	3.5	a00000673	20
117	0.8%H2/0.2%CO/1%O2/98%Ar	1351.0	1.6	a00000353	20	278	0.81%H2/4.03%O2/95.16%Ar	1360.0	4.2	a00000674	25
118	0.8%H2/0.2%CO/1%O2/98%Ar	980.0	1.6	a00000354	20	279	4.03%H2/20.16%O2/75.81%Ar	932.0	4.1	a00000675	40
119	0.5%H2/0.5%CO/1%O2/98%Ar	2004.0	1.6	a00000355	20	280	4.03%H2/20.16%O2/75.81%Ar	987.0	4.2	a00000676	30
120	0.5%H2/0.5%CO/1%O2/98%Ar	1273.0	1.6	a00000356	20	281	4.03%H2/20.16%O2/75.81%Ar	1021.0	4.2	a00000677	20
121	0.5%H2/0.5%CO/1%O2/98%Ar	992.0	1.6	a00000357	20	282	4.03%H2/20.16%O2/75.81%Ar	1131.0	4.1	a00000678	25
122	0.1%H2/0.9%CO/1%O2/98%Ar	1975.0	1.6	a00000358	20	283	12.54%H2/1.57%O2/85.89%Ar	967.0	4.0	a00000679	35
123	0.1%H2/0.9%CO/1%O2/98%Ar	1436.0	1.6	a00000359	20	284	12.54%H2/1.57%O2/85.89%Ar	997.0	4.1	a00000680	30
124	0.1%H2/0.9%CO/1%O2/98%Ar	1027.0	1.6	a00000360	20	285	12.54%H2/1.57%O2/85.89%Ar	1017.0	4.2	a00000681	20
125	0.444%H2/0.444%CO/0.223%H2O/0.889%O2/98%Ar	998.0	1.6	a00000489	50	286	12.54%H2/1.57%O2/85.89%Ar	1463.0	4.3	a00000682	25
126	0.444%H2/0.444%CO/0.223%H2O/0.889%O2/98%Ar	1146.0	1.6	a00000490	30	287	3.47%H2/3.47%O2/93.06%N2	1060.0	15.7	a00000683	35
127	8.91%H2/11.58%CO/10.25%O2/24.44%CO2/44.83%N2	981.0	1.2	a00000491	20	288	3.47%H2/3.47%O2/93.06%N2	1165.0	15.9	a00000684	25
128	8.91%H2/11.58%CO/10.25%O2/24.44%CO2/44.83%N2	1065.0	1.3	a00000492	20	289	3.47%H2/3.47%O2/93.06%N2	1243.0	16.2	a00000685	30
129	0.444%H2/0.444%CO/0.223%H2O/0.889%O2/98%Ar	1786.0	1.6	a00000493	30	290	0.81%H2/4.03%O2/95.16%Ar	1037.0	16.1	a00000686	40
130	8.91%H2/11.58%CO/10.25%O2/24.44%CO2/44.83%N2	1135.0	1.2	a00000494	20	291	0.81%H2/4.03%O2/95.16%Ar	1087.0	16.1	a00000687	30
131	8.91%H2/11.58%CO/10.25%O2/24.44%CO2/44.83%N2	975.0	1.7	a00000495	20	292	0.81%H2/4.03%O2/95.16%Ar	1141.0	16.3	a00000688	25
132	8.91%H2/11.58%CO/10.25%O2/24.44%CO2/44.83%N2	999.0	1.8	a00000496	20	293	0.81%H2/4.03%O2/95.16%Ar	1180.0	17.8	a00000689	25
133	8.91%H2/11.58%CO/10.25%O2/24.44%CO2/44.83%N2	1048.0	1.7	a00000497	20	294	0.81%H2/4.03%O2/95.16%Ar	1255.0	16.7	a00000690	30
134	0.444%H2/0.444%CO/0.223%H2O/0.889O2/98%Ar	1397.0	12.5	a00000498	30	295	4.03%H2/20.16%O2/75.81%Ar	956.0	18.7	a00000691	40
135	0.444%H2/0.444%CO/0.223%H2O/0.889O2/98%Ar	1284.0	12.5	a00000499	30	296	4.03%H2/20.16%O2/75.81%Ar	1010.0	18.1	a00000692	30
136	0.444%H2/0.444%CO/0.223%H2O/0.889O2/98%Ar	1100.0	12.5	a00000500	30	297	4.03%H2/20.16%O2/75.81%Ar	1142.0	17.8	a00000693	25
137	0.444%H2/0.444%CO/0.223%H2O/0.889O2/98%Ar	1299.0	32.0	a00000501	30	298	4.03%H2/20.16%O2/75.81%Ar	1178.0	17.6	a00000694	30
138	0.444%H2/0.444%CO/0.223%H2O/0.889O2/98%Ar	1186.0	32.0	a00000502	30	299	12.54%H2/1.57%O2/85.89%Ar	947.0	15.1	a00000695	45
139	0.46%H2/0.46%CO/0.15%CO2/0.39%O2/98%Ar	1883.0	1.6	a00000503	30	300	12.54%H2/1.57%O2/85.89%Ar	1100.0	15.5	a00000696	20

#	Mixture	T_5, K	P_5, bar	Attribute ID	Estimated error, %	#	Mixture	T, K	p, bar	Attribute ID	Estimated error, %
140	0.46%H2/0.46%CO/0.15%CO2/0.39%O2/98%Ar	1008.0	1.6	a00000504	50	301	12.54%H2/1.57%O2/85.89%Ar	1227.0	14.9	a00000697	25
141	0.46%H2/0.46%CO/0.15%CO2/0.39%O2/98%Ar	1360.0	12.5	a00000505	30	302	5.917%H2/2.959%O2/91.124%Ar	1456.7	1.3	a00000698	20
142	0.46%H2/0.46%CO/0.15%CO2/0.39%O2/98%Ar	1122.0	12.5	a00000506	30	303	5.917%H2/2.959%O2/91.124%Ar	1163.2	1.2	a00000699	20
143	0.46%H2/0.46%CO/0.15%CO2/0.39%O2/98%Ar	1291.0	32.0	a00000507	30	304	5.917%H2/2.959%O2/91.124%Ar	915.1	1.2	a00000700	25
144	0.46%H2/0.46%CO/0.15%CO2/0.39%O2/98%Ar	1233.0	32.0	a00000508	30	305	3.41%H2/3.41%O2/93.058%Ar	1193.6	5.0	a00000701	25
145	0.46%H2/0.46%CO/0.15%CO2/0.39%O2/98%Ar	1150.0	32.0	a00000509	30	306	3.41%H2/3.41%O2/93.058%Ar	1050.4	5.0	a00000702	25
146	0.5%H2/0.5%CO/1%O2/98%Ar	1763.0	1.6	a00000538	30	307	3.41%H2/3.41%O2/93.058%Ar	1022.1	5.0	a00000703	30
147	0.5%H2/0.5%CO/1%O2/98%Ar	1503.0	1.6	a00000539	25	308	3.41%H2/3.41%O2/93.058%Ar	1222.1	10.0	a00000704	30
148	0.5%H2/0.5%CO/1%O2/98%Ar	1068.0	1.6	a00000540	25	309	3.41%H2/3.41%O2/93.058%Ar	1122.3	10.0	a00000705	25
149	0.46%H2/0.46%CO/0.15%CO2/0.39%O2/98%Ar	1367.0	1.6	a00000542	30	310	3.41%H2/3.41%O2/93.058%Ar	1077.2	10.0	a00000706	25
150	0.46%H2/0.46%CO/0.15%CO2/0.39%O2/98%Ar	1199.0	12.5	a00000543	30	311	3.41%H2/3.41%O2/93.058%Ar	1041.5	10.0	a00000707	35
151	8.91%H2/11.58%CO/10.25%O2/24.44%CO2/44.83%N2	1017.0	1.9	a00000547	50	312	3.41%H2/3.41%O2/93.058%Ar	1036.1	10.0	a00000708	30
152	8.91%H2/11.58%CO/10.25%O2/24.44%CO2/44.83%N2	1024.0	2.6	a00000548	50	313	3.41%H2/3.41%O2/93.058%Ar	1267.2	20.0	a00000709	35
153	8.91%H2/11.58%CO/10.25%O2/24.44%CO2/44.83%N2	1054.0	2.4	a00000549	30	314	3.41%H2/3.41%O2/93.058%Ar	1168.8	20.0	a00000710	30
154	8.91%H2/11.58%CO/10.25%O2/24.44%CO2/44.83%N2	1091.0	2.3	a00000550	30	315	3.41%H2/3.41%O2/93.058%Ar	1092.7	20.0	a00000711	35
155	2.81%H2/1.19%CO/2%O2/94%Ar	1161.2	1.5	a00000551	35	316	3.41%H2/3.41%O2/93.058%Ar	1009.4	20.0	a00000712	40
156	2.81%H2/1.19%CO/2%O2/94%Ar	1025.0	1.7	a00000552	25	317	30%H2/14.8%O2/55.2%N2	1179.7	2.0	a00000713	35
157	2.81%H2/1.19%CO/2%O2/94%Ar	978.5	1.7	a00000553	40	318	30%H2/14.8%O2/55.2%N2	1077.3	2.0	a00000714	35
158	2.81%H2/1.19%CO/2%O2/94%Ar	944.8	1.9	a00000554	50	319	30%H2/14.8%O2/55.2%N2	1025.8	2.0	a00000715	30
159	2.81%H2/1.19%CO/2%O2/94%Ar	932.9	1.9	a00000555	45	320	30%H2/14.8%O2/55.2%N2	994.4	2.0	a00000716	35
160	2.81%H2/1.19%CO/2%O2/94%Ar	902.1	1.8	a00000556	90	321	30%H2/14.8%O2/55.2%N2	986.6	2.0	a00000717	35
161	2.81%H2/1.19%CO/2%O2/94%Ar	1178.8	9.1	a00000557	25						

Appendix 2. Laminar flame speed QoIs

#	Mixture	T_0, K	P, bar	φ	Estimated error, %	#	Mixture	T_0, K	P, bar	φ	Estimated error, %
1	50/50% CO/H2/air	300	1	0.8	10	80	85%H2-15%CO/11%O2-89%He	298	1	0.6	10
2	50/50% CO/H2/air	300	1	1.2	10	81	85%H2-15%CO/11%O2-89%He	298	5	0.6	10
3	50/50% CO/H2/air	300	1	2.5	15	82	75/25% CO/H2/He, O2/He=1:6, 10% dil. with CO2	298	5	0.8	10
4	50/50% CO/H2/air	300	1	4	20	83	75/25% CO/H2/He, O2/He=1:6, 30% dil. with CO2	298	5	0.8	10
5	50/50% CO/H2/air	300	2	0.6	20	84	75/25% CO/H2/He, O2/He=1:6, 10% dil. with CO2	298	10	0.8	10
6	50/50% CO/H2/air	300	2	1.4	10	85	75/25% CO/H2/He, O2/He=1:6, 30% dil. with CO2	298	10	0.8	10
7	50/50% CO/H2/air	300	2	2	10	86	40%/40%/20% CO/H2/CO2	295	1	0.6	10
8	50/50% CO/H2/air	300	2	4	20	87	40%/40%/20% CO/H2/CO2	295	1	1.4	10
9	95/5% CO/H2/He	300	5	1.2	10	88	40%/40%/20% CO/H2/CO2	295	1	1.8	10
10	95/5% CO/H2/He	300	5	1.4	10	89	40%/40%/20% CO/H2/CO2	295	1	2.2	15
11	95/5% CO/H2/He	300	5	2	15	90	70/30% CO/H2/air, 10% dil. with CO2	295	1	1	10
12	95/5% CO/H2/He	300	5	3.5	20	91	70/30% CO/H2/air, 60% dil. with CO2	295	1	1	10
13	95/5% CO/H2/He	300	10	0.75	15	92	70/30% CO/H2/air, 10% dil. with CO2	295	1	0.6	10
14	95/5% CO/H2/He	300	10	1.2	15	93	70/30% CO/H2/air, 60% dil. with CO2	295	1	0.6	10
15	95/5% CO/H2/He	300	10	1.4	15	94	30/70% CO/H2/air, 10% dil. with CO2	295	1	1	10
16	95/5% CO/H2/He	300	10	1.8	15	95	30/70% CO/H2/air, 60% dil. with CO2	295	1	1	10
17	95/5% CO/H2/He	300	10	3.5	25	96	30/70% CO/H2/air, 10% dil. with CO2	295	1	0.6	10
18	95/5% CO/H2/He	300	20	1	20	97	30/70% CO/H2/air, 60% dil. with CO2	295	1	0.6	10
19	95/5% CO/H2/He	300	20	1.4	20	98	50/50% CO/H2/air, 10% dil. with CO2	295	1	1	10
20	95/5% CO/H2/He	300	20	2	20	99	50/50% CO/H2/air, 60% dil. with CO2	295	1	1	10
21	95/5% CO/H2/He	300	20	3.5	25	100	50%H2-50%CO/O2-47%H2O	400	1	0.6	10
22	95/5% CO/H2/He	300	40	1.2	20	101	50%H2-50%CO/O2-47%H2O	400	1	1.2	10

#	Mixture	T_0, K	P, bar	φ	Estimated error, %	#	Mixture	T_0, K	P, bar	φ	Estimated error, %
23	95/5% CO/H2/He	300	40	1.4	20	102	50%H2-50%CO/O2-47%H2O	400	1	2	10
24	95/5% CO/H2/He	300	40	2	20	103	95/5% CO/H2/air	298	1	2	10
25	95/5% CO/H2/He	300	40	3	25	104	95/5% CO/H2/air	298	1	2.4	15
26	95/5% CO/H2/air	300	1	0.6	15	105	50/50% CO/H2/air diluted with 20% N2	298	1	1	10
27	95/5% CO/H2/air	300	1	1	20	106	50/50% CO/H2/air diluted with 20% N2	298	1	1.8	10
28	95/5% CO/H2/air	300	1	1.5	20	107	50/50% CO/H2/air diluted with 20% N2	298	1	4.2	20
29	95/5% CO/H2/air	300	1	2.5	15	108	50/50% CO/H2/air diluted with 60% N2	298	1	0.8	10
30	95/5% CO/H2/air	300	1	4	20	109	50/50% CO/H2/air diluted with 60% N2	298	1	1.4	10
31	95/5% CO/H2/air	300	1	6	20	110	50/50% CO/H2/air diluted with 60% N2	298	1	2.2	15
32	95/5% CO/H2/air	300	2	1	10	111	5%H2-95%CO,O2, 30% dil. with N2	298	1	0.6	10
33	95/5% CO/H2/air	300	2	2.5	15	112	5%H2-95%CO,O2, 30% dil. with N2	298	1	1.2	10
34	95/5% CO/H2/air	300	2	4	20	113	5%H2-95%CO,O2, 30% dil. with N2	298	1	2	10
35	50/50% CO/H2/He	300	5	1	10	114	50%H2-50%CO,O2, 50% dil. with N2	298	1	0.6	10
36	50/50% CO/H2/He	300	5	1.8	10	115	50%H2-50%CO,O2, 50% dil. with N2	298	1	1.2	10
37	50/50% CO/H2/He	300	5	3.5	20	116	50%H2-50%CO,O2, 50% dil. with N2	298	1	2	10
38	50/50% CO/H2/He	300	10	1	15	117	95%CO-5%H2/air/H2O, H2O=20%	373	1	1.2	10
39	50/50% CO/H2/He	300	10	1.8	15	118	95%/5%CO/H2/ air ZH2O=20%	373	1	2	10
40	50/50% CO/H2/He	300	10	3.5	25	119	95%/5%CO/H2/ air ZH2O=20%	373	1	3	15
41	95/5% CO/H2/air	300	0.5	0.8	10	120	50%/50%CO/H2/ air ZH2O=20%	373	5	0.8	10
42	95/5% CO/H2/air	300	0.5	1	10	121	50%/50%CO/H2/ air ZH2O=20%	373	5	1.5	10
43	95/5% CO/H2/air	300	0.5	1.6	10	122	50%CO-50%H2/air/H2O, H2O=20%	373	5	2.5	15
44	95/5% CO/H2/air	300	0.5	3	15	123	50%H2-50%CO/air, CO2=0.15	373	1	0.8	10
45	95/5% CO/H2/air	300	0.5	4.5	20	124	50%H2-50%CO/air, CO2=0.15	373	1	2	10
46	95/5% CO/H2/air	300	4	0.6	10	125	50%H2-50%CO/air, CO2=0.15	373	1	3	15
47	95/5% CO/H2/air	300	4	1.6	10	126	50%H2-50%CO/air, H2O=0.15	373	1	0.8	10
48	95/5% CO/H2/air	300	4	2.4	15	127	50%H2-50%CO/air, H2O=0.15	373	1	2	10
49	95/5% CO/H2/air	300	4	5	20	128	50%H2-50%CO/air, H2O=0.15	373	1	3	15
50	50/50% CO/H2/air	500	1	0.63	10	129	H2/air	298	1	0.5	10
51	50/50% CO/H2/air	500	1	1.01	10	130	H2/air	298	1	1.5	10
52	50/50% CO/H2/air	700	1	0.63	10	131	H2/air	298	1	4.5	20
53	50/50% CO/H2/air	700	1	0.73	10	132	H2/O2/Ar, O2/(O2+Ar)=21%	298	1	0.6	10
54	50/50% CO/H2/air	700	1	0.9	10	133	H2/O2/Ar, O2/(O2+Ar)=21%	298	1	1.8	10
55	80/20% CO/H2/He	600	15	0.6	20	134	H2/O2/Ar, O2/(O2+Ar)=21%	298	1	4.5	20
56	50/50% CO/H2/He	600	15	0.6	20	135	H2/O2/He, O2/(O2+He)=21%	298	1	0.6	10
57	20/80% CO/H2/He	600	15	0.6	20	136	H2/O2/He, O2/(O2+He)=21%	298	1	1.8	10
58	95/5% CO/H2/air, 0% dil. with H20	323	1	0.6	10	137	H2/O2/He, O2/(O2+He)=21%	298	1	4.5	20
59	95/5% CO/H2/air, 15% dil. with H20	323	1	0.6	10	138	H2/O2/He, O2/(O2+He)=0.125	298	3	0.6	10
60	95/5% CO/H2/air, 35% dil. with H20	323	1	0.6	10	139	H2/O2/He, O2/(O2+He)=0.125	298	3	1.5	10
61	95/5% CO/H2/air, 0% dil. with H20	323	1	0.9	10	140	H2/O2/He, O2/(O2+He)=0.125	298	3	3.5	20
62	95/5% CO/H2/air, 15% dil. with H20	323	1	0.9	10	141	H2/O2/He, O2/(O2+He)=0.125	298	5	0.5	10
63	95/5% CO/H2/air, 35% dil. with H20	323	1	0.9	10	142	H2/O2/He, O2/(O2+He)=0.125	298	5	1.5	10
64	80/20% CO/H2/air, 0% dil. with H20	323	1	0.6	10	143	H2/O2/He, O2/(O2+He)=0.125	298	5	3.5	20
65	80/20% CO/H2/air, 15% dil. with H20	323	1	0.6	10	144	H2/O2/He, O2/(O2+He)=0.08	298	10	0.75	10
66	80/20% CO/H2/air, 35% dil. with H20	323	1	0.6	10	145	H2/O2/He, O2/(O2+He)=0.08	298	10	1.25	10
67	50%H2-50%CO/90%He-10%O2	298	1	0.7	10	146	H2/O2/He, O2/(O2+He)=0.08	298	10	2	10
68	50%H2-50%CO/90%He-10%O2	298	5	0.7	10	147	H2/O2/He, O2/(O2+He)=0.08	298	15	0.75	10
69	50%H2-50%CO/90%N2-10%O2	298	1	1	10	148	H2/O2/He, O2/(O2+He)=0.08	298	15	1.5	10
70	50%H2-50%CO/90%N2-10%O2	298	3	1	10	149	H2/O2/He, O2/(O2+He)=0.08	298	15	2	10
71	50%H2-50%CO/87.5%He-12.5%O2	298	1	0.6	10	150	H2/O2/He, O2/(O2+He)=0.08	298	20	0.75	10

#	Mixture	T_0, K	P, bar	φ	Estimated error, %	#	Mixture	T_0, K	P, bar	φ	Estimated error, %
72	50%H2-50%CO/87.5%He-12.5%O2	298	3	0.6	10	151	H2/O2/He, O2/(O2+He)=0.08	298	20	1.5	10
73	50%H2-50%CO/87.5%He-12.5%O2	298	9	0.6	15	152	H2/O2/He, O2/(O2+He)=0.08	298	20	2	10
74	85%H2-15%CO/12.5%O2-87.5%He	298	1	0.5	10	153	H2/O2, 50% CO2 dil.	298	1	0.6	10
75	85%H2-15%CO/12.5%O2-87.5%He	298	5	0.5	10	154	H2/O2, 50% CO2 dil.	298	1	1.2	10
76	85%H2-15%CO/12.5%O2-87.5%He	298	10	0.5	15	155	H2/O2, 50% CO2 dil.	298	1	2	10
77	85%H2-15%CO/12.5%O2-87.5%He	298	1	0.5	10	156	H2/O2, 50% N2 dil.	298	1	0.6	10
78	85%H2-15%CO/12.5%O2-87.5%He	298	4	0.5	10	157	H2/O2, 50% N2 dil.	298	1	1.2	10
79	85%H2-15%CO/12.5%O2-87.5%He	298	10	0.5	15	158	H2/O2, 50% N2 dil.	298	1	2	10

Appendix 3. List of QoIs suggested by VCM

Ignition delay QoIs											
#	Target ID	LB change, ms	UB change, ms	#	Target ID	LB change, ms	UB change, ms	#	Target ID	LB change, ms	UB change, ms
1	a00000110	-0.4774	0.0000	29	a00000498	-0.0017	0.0000	57	a00000540	0.0000	0.1910
2	a00000194	-0.1406	0.0000	30	a00000491	-0.6858	0.0000	58	a00000552	0.0000	0.0261
3	a00000228	-0.2355	0.0000	31	a00000492	-0.0097	0.0000	59	a00000555	0.0000	0.5183
4	a00000235	-0.5238	0.0000	32	a00000495	-0.5137	0.0000	60	a00000570	0.0000	0.0719
5	a00000236	-0.3754	0.0000	33	a00000496	-0.3855	0.0000	61	a00000580	0.0000	1.1304
6	a00000237	-0.2418	0.0000	34	a00000497	-0.0217	0.0000	62	a00000591	0.0000	0.0795
7	a00000240	-0.0606	0.0000	35	a00000150	0.0000	0.0709	63	a00000592	0.0000	0.1835
8	a00000243	-0.0077	0.0000	36	a00000152	0.0000	0.0262	64	a00000593	0.0000	0.2893
9	a00000318	-0.1501	0.0000	37	a00000153	0.0000	0.0026	65	a00000595	0.0000	1.1639
10	a00000547	-0.1812	0.0000	38	a00000154	0.0000	0.0417	66	a00000600	0.0000	2.4465
11	a00000548	-0.0016	0.0000	39	a00000155	0.0000	0.0472	67	a00000612	0.0000	6.4691
12	a00000549	-0.1356	0.0000	40	a00000107	0.0000	0.0052	68	a00000619	0.0000	3.8471
13	a00000558	-0.0035	0.0000	41	a00000136	0.0000	0.0051	69	a00000620	0.0000	0.0071
14	a00000582	-0.0360	0.0000	42	a00000179	0.0000	0.8560	70	a00000631	0.0000	2.8933
15	a00000623	-0.3518	0.0000	43	a00000186	0.0000	0.0097	71	a00000644	0.0000	0.0068
16	a00000624	-0.5036	0.0000	44	a00000191	0.0000	9.1044	72	a00000645	0.0000	0.0029
17	a00000633	-0.0073	0.0000	45	a00000196	0.0000	0.0043	73	a00000653	0.0000	0.0002
18	a00000635	-0.1842	0.0000	46	a00000310	0.0000	0.9045	74	a00000673	0.0000	0.0336
19	a00000647	-0.4052	0.0000	47	a00000311	0.0000	0.0128	75	a00000686	0.0000	13.2658
20	a00000649	-0.0042	0.0000	48	a00000312	0.0000	0.0136	76	a00000692	0.0000	0.5164
21	a00000650	-0.1770	0.0000	49	a00000316	0.0000	2.8089	77	a00000698	0.0000	0.0014
22	a00000662	-0.0034	0.0000	50	a00000322	0.0000	1.6876	78	a00000699	0.0000	0.0000
23	a00000663	-0.1294	0.0000	51	a00000335	0.0000	0.0052	79	a00000700	0.0000	1.3386
24	a00000664	-0.0087	0.0000	52	a00000353	0.0000	0.0406	80	a00000704	0.0000	0.0061
25	a00000665	-0.0024	0.0000	53	a00000354	0.0000	0.8257	81	a00000710	0.0000	0.0119
26	a00000677	-0.1225	0.0000	54	a00000356	0.0000	0.0408	82	a00000608	0.0000	0.0007
27	a00000682	-0.0011	0.0000	55	a00000357	0.0000	0.5274	83	a00000713	0.0000	0.0001
28	a00000703	-0.0800	0.0000	56	a00000538	0.0000	0.0150	84	a00000505	0.0000	0.0118
Laminar flame speed QoIs											
#	Flame ID	LB change, cm/s	UB change, cm/s	#	Flame ID	LB change, cm/s	UB change, cm/s	#	Flame ID	LB change, cm/s	UB change, cm/s
1	Flame QoI 67	0.0000	0.1786	2	Flame QoI 68	-3.8602	0.0000	3	Flame QoI 112	0.0000	1.7301

Acknowledgments

The authors from the University of California, Berkeley, acknowledge the support of the National Nuclear Security Administration, U.S. Department of Energy, under Award DE-NA0002375. The views and opinions of authors expressed herein do not necessarily state or reflect those of the United States Government or any agency thereof.

References

[1]Frenklach, M. "Transforming data into knowledge—Process Informatics for combustion chemistry," *Proc. Combust. Inst.* Vol. 31, No. 1, 2007, pp. 125-140.

[2]Frenklach, M., Packard, A., and Feeley, R. "Optimization of reaction models with Solution Mapping," *Modeling of Chemical Reactions*. Elsevier, New York, 2007, pp. 243–291.

[3]Smith, G. P., Golden, D. M., Frenklach, M., Moriarty, N. W., Eiteneer, B., Goldenberg, M., Bowman, T., Hanson, R. K., Song, S., Gardiner, W. C., Jr., Lissianski, V. V., and Qin, Z. "GRI-Mech 3.0," http://www.me.berkeley.edu/gri_mech/.

[4]Kéromnès, A., Metcalfe, W. K., Heufer, K. A., Donohoe, N., Das, A. K., Sung, C.-J., Herzler, J., Naumann, C., Griebel, P., Mathieu, O., Krejci, M. C., Petersen, E. L., Pitz, W. J., and Curran, H. J. "An experimental and detailed chemical kinetic modeling study of hydrogen and syngas mixture oxidation at elevated pressures," *Combust. Flame* Vol. 160, No. 6, 2013, pp. 995-1011.

[5]Turányi, T., Nagy, T., Zsély, I. G., Cserháti, M., Varga, T., Szabó, B. T., Sedyó, I., Kiss, P. T., Zempléni, A., and Curran, H. J. "Determination of rate parameters based on both direct and indirect measurements," *Int. J. Chem. Kinet.* Vol. 44, No. 5, 2012, pp. 284-302.

[6]Varga, T., Olm, C., Nagy, T., Zsély, I. G., Valkó, É., Pálvölgyi, R., Curran, H. J., and Turányi, T. "Development of a joint hydrogen and syngas combustion mechanism based on an optimization approach," *Int. J. Chem. Kinet.* Vol. 48, No. 8, 2016, pp. 407-422.

[7]Frenklach, M. "PrIMe," https://prime.cki-know.org/.

[8]Frenklach, M., Packard, A., Seiler, P., and Feeley, R. "Collaborative data processing in developing predictive models of complex reaction systems," *Int. J. Chem. Kinet.* Vol. 36, No. 1, 2004, pp. 57-66.

[9]You, X., Packard, A., and Frenklach, M. "Process informatics tools for predictive modeling: Hydrogen combustion," *Int. J. Chem. Kinet.* Vol. 44, No. 2, 2012, pp. 101-116.

[10]Slavinskaya, N. A., Abbasi, M., Starcke, J. H., Whitside, R., Mirzayeva, A., Riedel, U., Li, W., Oreluk, J., Hegde, A., Packard, A., Frenklach, M., Gerasimov, G., and Shatalov, O. "Development of an Uncertainty Quantification Predictive Chemical Reaction Model for Syngas Combustion," *Energy & Fuels* Vol. 31, No. 3, 2017, pp. 2274-2297.

[11]Feeley, R., Seiler, P., Packard, A., and Frenklach, M. "Consistency of a reaction dataset," *J. Phys. Chem. A* Vol. 108, No. 44, 2004, pp. 9573-9583.

[12]Russi, T., Packard, A., Feeley, R., and Frenklach, M. "Sensitivity analysis of uncertainty in model prediction," *J. Phys. Chem. A* Vol. 112, No. 12, 2008, pp. 2579-2588.

[13]Russi, T., Packard, A., and Frenklach, M. "Uncertainty quantification: Making predictions of complex reaction systems reliable," *Chem. Phys. Lett.* Vol. 499, No. 1-3, 2010, pp. 1-8.

[14]Seiler, P., Frenklach, M., Packard, A., and Feeley, R. "Numerical approaches for collaborative data processing," *Optim. Eng.* Vol. 7, No. 4, 2006, pp. 459-478.

[15]Frenklach, M., Packard, A., and Seiler, P. "Prediction uncertainty from models and data," *IEEE*. Anchorage, Alaska, 2002, pp. 4135-4140.

[16]Hegde, A., Li, W., Oreluk, J., Packard, A., and Frenklach, M. "Consistency analysis for massively inconsistent datasets in Bound-to-Bound Data Collaboration." preparation.

[17]You, X., Russi, T., Packard, A., and Frenklach, M. "Optimization of combustion kinetic models on a feasible set," *Proc. Combust. Inst.* Vol. 33, No. 1, 2011, pp. 509-516.

[18]Wang, H., and Sheen, D. A. "Combustion kinetic model uncertainty quantification, propagation and minimization," *Prog. Energy Combust. Sci.* Vol. 47, 2015, pp. 1-31.

[19]Frenklach, M. "Modeling," *Combustion Chemistry*. Springer-Verlag, New York, 1984, pp. 423-453.

[20]Kalitan, D. M., Mertens, J. D., Crofton, M. W., and Petersen, E. L. "Ignition and oxidation of lean CO/H_2 fuel blends in air," *J. Propul. Power* Vol. 23, No. 6, 2007, pp. 1291-1301.

[21]Mathieu, O., Kopp, M. M., and Petersen, E. L. "Shock-tube study of the ignition of multi-component syngas mixtures with and without ammonia impurities," *Proc. Combust. Inst.* Vol. 34, No. 2, 2013, pp. 3211-3218.

[22]Herzler, J., and Naumann, C. "Shock-tube study of the ignition of methane/ethane/hydrogen mixtures with hydrogen contents from 0% to 100% at different pressures," *Proceedings of the Combustion Institute* Vol. 32, No. 1, 2009, pp. 213-220.

[23]Petersen, E. L., Kalitan, D. M., Barrett, A. B., Reehal, S. C., Mertens, J. D., Beerer, D. J., Hack, R. L., and McDonell, V. G. "New syngas/air ignition data at lower temperature and elevated pressure and comparison to current kinetics models," *Combust. Flame* Vol. 149, No. 1-2, 2007, pp. 244-247.

[24]Vasu, S. S., Davidson, D. F., and Hanson, R. K. "Shock tube study of syngas ignition in rich CO_2 mixtures and determination of the rate of $H + O_2 + CO_2 \rightarrow HO_2 + CO_2$," *Energy Fuels* Vol. 25, No. 3, 2011, pp. 990-997.

[25]Naumann, C., Herzler, J., Griebel, P., Curran, H. J., Keromnes, A., and Mantzaras, I. "Low Emission Gas Turbine Technology for Hydrogen-rich Syngas. H2-IGCC project - Deliverable 1.1.3 report.," *7th Framework Programme FP7-ENERGY-2008-TREN-1, ENERGY-2008-6-CLEAN COAL TECHNOLOGIES*. 2011.

[26]Mertens, J. D., Kalitan, D. M., Barrett, A. B., and Petersen, E. L. "Determination of the rate of $H+O_2+M \rightarrow HO_2+M$ ($M=N_2$, Ar, H_2O) from ignition of syngas at practical conditions," *Proc. Combust. Inst.* Vol. 32, No. 1, 2009, pp. 295-303.

[27]Thi, L. D., Zhang, Y., and Huang, Z. "Shock tube study on ignition delay of multi-component syngas mixtures – Effect of equivalence ratio," *Int. J. Hydrogen Energy* Vol. 39, No. 11, 2014, pp. 6034-6043.

[28]Pan, L., Zhang, Y., Zhang, J., Tian, Z., and Huang, Z. "Shock tube and kinetic study of C2H6/H2/O2/Ar mixtures at elevated pressures," *International Journal of Hydrogen Energy* Vol. 39, No. 11, 2014, pp. 6024-6033.

[29]Mittal, G., Sung, C.-J., and Yetter, R. A. "Autoignition of H_2/CO at elevated pressures in a rapid compression machine," *Int. J. Chem. Kinet.* Vol. 38, No. 8, 2006, pp. 516-529.

[30]Schultz, E. S., J. "Validation of Detailed Reaction Mechanisms for Detonation Simulation," *Explosion Dynamics Laboratory Report FM99-5*. California Institute of Technology, Pasadena, CA, 2000.

[31]Petersen, E. L. D., D.F.; Rohrig, M.; Hanson, R.K. "High pressure shock tube measurements of ignition times in stoichiometric H_2/O_2/Ar mixtures," *20th International symposium on shock waves*. 1996, pp. 941–6.

[32]Zhang, Y., Huang, Z., Wei, L., Zhang, J., and Law, C. K. "Experimental and modeling study on ignition delays of lean mixtures of methane, hydrogen, oxygen, and argon at elevated pressures," *Combustion and Flame* Vol. 159, No. 3, 2012, pp. 918-931.

[33]Herzler, J., and Naumann, C. "Shock tube study of the ignition of lean CO/H_2 fuel blends at intermediate temperatures and high pressure," *Combust. Sci. Technol.* Vol. 180, No. 10-11, 2008, pp. 2015-2028.

[34]Pang, G. A., Davidson, D. F., and Hanson, R. K. "Experimental study and modeling of shock tube ignition delay times for hydrogen–oxygen–argon mixtures at low temperatures," *Proceedings of the Combustion Institute* Vol. 32, No. 1, 2009, pp. 181-188.

[35]Slack, M. W. "Rate Coefficient for H + O_2 + M = HO_2 + M Evaluated from Shock Tube Measurements of Induction Times," *Combustion and Flame* Vol. 28, 1977, pp. 241-249.

[36]Krejci, M. C., Mathieu, O., Vissotski, A. J., Ravi, S., Sikes, T. G., Petersen, E. L., Kérmonès, A., Metcalfe, W., and Curran, H. J. "Laminar flame speed and ignition delay time data for the kinetic modeling of hydrogen and syngas fuel blends," *J. Eng. Gas Turbines Power* Vol. 135, No. 2, 2013, p. 021503.

[37]Sun, H., Yang, S. I., Jomaas, G., and Law, C. K. "High-pressure laminar flame speeds and kinetic modeling of carbon monoxide/hydrogen combustion," *Proc. Combust. Inst.* Vol. 31, No. 1, 2007, pp. 439-446.

[38]Goswami, M., van Griensven, J. G. H., Bastiaans, R. J. M., Konnov, A. A., and Goey, L. P. H. "Experimental and modeling study of the effect of elevated pressure on lean high-hydrogen syngas flames," *Proc. Combust. Inst.* Vol. 35, No. 1, 2015, pp. 655-662.

[39]Wang, Z. H., Weng, W. B., He, Y., Li, Z. S., and Cen, K. F. "Effect of H_2/CO ratio and N_2/CO_2 dilution rate on laminar burning velocity of syngas investigated by direct measurement and simulation," *Fuel* Vol. 141, 2015, pp. 285-292.

[40]Hassan, M. I., Aung, K. T., and Faeth, G. M. "Properties of Laminar Premixed CO/H/Air Flames at Various Pressures," *J. Propul. Power* Vol. 13, No. 2, 1997, pp. 239-245.

[41]Zhang, W., Gou, X., Kong, W., and Chen, Z. "Laminar flame speeds of lean high-hydrogen syngas at normal and elevated pressures," *Fuel* Vol. 181, 2016, pp. 958-963.

[42]Weng, W. B., Wang, Z. H., He, Y., Whiddon, R., Zhou, Y. J., Li, Z. S., and Cen, K. F. "Effect of N_2/CO_2 dilution on laminar burning velocity of H_2–CO–O_2 oxy-fuel premixed flame," *Int. J. Hydrogen Energy* Vol. 40, No. 2, 2015, pp. 1203-1211.

[43]Natarajan, J., Lieuwen, T., and Seitzman, J. "Laminar flame speeds of H_2/CO mixtures: Effect of CO_2 dilution, preheat temperature, and pressure," *Combust. Flame* Vol. 151, No. 1-2, 2007, pp. 104-119.

[44]Han, M., Ai, Y., Chen, Z., and Kong, W. "Laminar flame speeds of H_2/CO with CO_2 dilution at normal and elevated pressures and temperatures," *Fuel* Vol. 148, 2015, pp. 32-38.

[45]Xie, Y., Wang, J., Xu, N., Yu, S., Zhang, M., and Huang, Z. "Thermal and chemical effects of water addition on laminar burning velocity of syngas," *Energy Fuels* Vol. 28, No. 5, 2014, pp. 3391-3398.

[46]Natarajan, J., Kochar, Y., Lieuwen, T., and Seitzman, J. "Pressure and preheat dependence of laminar flame speeds of $H_2/CO/CO_2/O_2$/He mixtures," *Proc. Combust. Inst.* Vol. 32, No. 1, 2009, pp. 1261-1268.

[47]Lapalme, D., and Seers, P. "Influence of CO_2, CH_4, and initial temperature on H_2/CO laminar flame speed," *Int. J. Hydrogen Energy* Vol. 39, No. 7, 2014, pp. 3477-3486.

[48]Xie, Y., Wang, J., Xu, N., Yu, S., and Huang, Z. "Comparative study on the effect of CO_2 and H_2O dilution on laminar burning characteristics of CO/H_2/air mixtures," *Int. J. Hydrogen Energy* Vol. 39, No. 7, 2014, pp. 3450-3458.

[49]Das, A. K., Kumar, K., and Sung, C.-J. "Laminar flame speeds of moist syngas mixtures," *Combust. Flame* Vol. 158, No. 2, 2011, pp. 345-353.

[50]Li, H.-M., Li, G.-X., Sun, Z.-Y., Zhou, Z.-H., Li, Y., and Yuan, Y. "Effect of dilution on laminar burning characteristics of $H_2/CO/CO_2$/air premixed flames with various hydrogen fractions," *Exp. Therm. Fluid Sci.* Vol. 74, 2016, pp. 160-168.

[51]Aung, K. T., Hassan, M. I., and Faeth, G. M. "Flame Stretch Interactions of Laminar Premixed Hydrogen/Air Flames at Normal Temperature and Pressure," *Combust. Flame* Vol. 109, 1997, pp. 1-24.

[52]Taylor, S. C. "Burning Velocity and the Influence of Flame Stretch." Ph.D. thesis, University of Leeds, 1991.

[53]Egolfopoulos, F. N., and Law, C. K. "An experimental and computational study of the burning rates of ultra-lean to moderately-rich H2/O2/N2 laminar flames with pressure variations," *Proc. Combust. Inst.* Vol. 23, 1990, p. 333.

[54]Law, C. K. "A Compilation of Experimental Data on Laminar Burning Velocities," *Reduced Kinetic Mechanisms for Applications in Combustion Systems* Springer-Verlag, Berlin, 1993, p. 15.

[55]Vagelopoulos, C. M., Egolfopoulos, F. N., and Law, C. K. "Further considerations on the determination of laminar flame speeds with the counterflow twin-flame technique," *Proc. Combust. Inst.* Vol. 25, No. 1, 1994, pp. 1341-1347.

[56]Hu, E., Huang, Z., He, J., Jin, C., and Zheng, J. "Experimental and numerical study on laminar burning characteristics of premixed methane–hydrogen–air flames," *International Journal of Hydrogen Energy* Vol. 34, No. 11, 2009, pp. 4876-4888.

[57]Tang, C., Huang, Z., Jin, C., He, J., Wang, J., Wang, X., and Miao, H. "Laminar burning velocities and combustion characteristics of propane–hydrogen–air premixed flames," *International Journal of Hydrogen Energy* Vol. 33, No. 18, 2008, pp. 4906-4914.

[58]Verhelst, S., Woolley, R., Lawes, M., and Sierens, R. "Laminar and unstable burning velocities and Markstein lengths of hydrogen–air mixtures at engine-like conditions," *Proceedings of the Combustion Institute* Vol. 30, No. 1, 2005, pp. 209-216.

[59]Kwon, O. C., and Faeth, G. M. "Flame/stretch interactions of premixed hydrogen-fueled flames: Measurements and predictions," *Combust. Flame* Vol. 124, No. 4, 2001, pp. 590-610.

[60]Tse, S. D., Zhu, D. L., and Law, C. K. "Morphology and burning rates of expanding spherical flames in H_2/O_2/inert mixtures up to 60 atmospheres," *Proc. Combust. Inst.* Vol. 28, 2000, p. 1793.

[61]Goswami, M., Bastiaans, R. J. M., Konnov, A. A., and Goey, L. P. H. "Laminar burning velocity of lean H_2–CO mixtures at elevated pressure using the heat flux method," *Int. J. Hydrogen Energy* Vol. 39, No. 3, 2014, pp. 1485-1498.

[62]Sun, S., Meng, S., Zhao, Y., Xu, H., Guo, Y., and Qin, Y. "Experimental and theoretical studies of laminar flame speed of CO/H_2 in O_2/H_2O atmosphere," *Int. J. Hydrogen Energy* Vol. 41, No. 4, 2016, pp. 3272-3283.